Platinacycles Containing a Primary Amine Platinum(II) Compounds for Treating Cisplatin-Resistant Cancers by Oxidant Therapy

Miguel Clemente,[†] Ibrahim Halil Polat,[‡,∇] Joan Albert,[†] Ramon Bosque,[†] Margarita Crespo,[†] Jaume Granell,[*,†] Concepción López,[†] Manuel Martínez,[†] Josefina Quirante,[*,§] Ramon Messeguer,[⊥] Carme Calvis,[⊥] Josefa Badía,[‖,∇] Laura Baldomà,[‖,∇] Mercè Font-Bardia,[#] and Marta Cascante[‡,∇,○]

†Departament de Química Inorgànica i Orgànica, Secció de Química Inorgànica, Facultat de Química, ‡Department of Biochemistry and Molecular Biomedicine, Faculty of Biology, Unit Associated with CSIC, §Laboratori de Química Orgànica, Facultat de Farmàcia,and ‖Departament de Bioquímica i Biologia Molecular, Facultat de Farmàcia, Universitat de Barcelona, 08028 Barcelona, Spain
⊥Biomed Division LEITAT Technological Center, Parc Científic, Edifici Hèlix, Baldiri Reixach, 15-21, 08028 Barcelona, Spain
#Unitat de Difracció de RX, Centres Científics i Tecnològics de la Universitat de Barcelona (CCiTUB), Solé i Sabarís 1-3. 08028 Barcelona, Spain
∇Institut de Biomedicina, Universitat de Barcelona, Institut de Recerca Sant Joan de Déu, 08028 Barcelona, Spain
○Centro de Investigación Biomédica en Red de Enfermedades Hepáticas y Digestivas (CIBEREHD), Instituto de Salud Carlos III (ISCIII), 28020 Madrid, Spain

ABSTRACT:

Cisplatin is an efficient anticancer drug, but its effects are often lost after several chemotherapy cycles, showing important secondary effects. For these reasons, new anticancer agents, with different coordination properties and mechanisms of action, are needed. Here we describe the reaction of 2-phenylaniline with cis-[PtCl2(dmso)2] and sodium acetate to afford a cycloplatinated compound 2 and the synthesis and some biological studies of 3−6 (two neutral and two ionic compounds): [PtCl(C−N)(L)], C−N cycloplatinated 2-phenylaniline with L = PPh3 (3) or P(4-FC6H4)3 (4) and [Pt(C−N)-(L-L)]Cl with L-L = Ph2PCH2CH2Ph2 (5) or (C6F5)2PCH2-CH2(C6F5)2 (6). Ionic platinacycles 5 and 6 show a greater antiproliferative activity than that of cisplatin in human lung, breast, and colon cancer cell lines (A-549, MDA-MB-231 and MCF-7, and HCT-116), a remarkable result given the fact that they do not show covalent interaction with DNA. 5 and 6 have also been found able to oxidize NADH by a catalytic process prododucing H2O2 as ROS. The activity of these complexes to generate ROS seems to be the key factor to explain their potent anticancer activity; it should be noted that platinum(II) complexes showing biocatalytic activity for hydride transfer from NADH have not been described so far. Ionic complex 6 shows low affinity to some target proteins; the presence of perfluoroaromatic rings seems to hinder its interaction with some biomolecules.

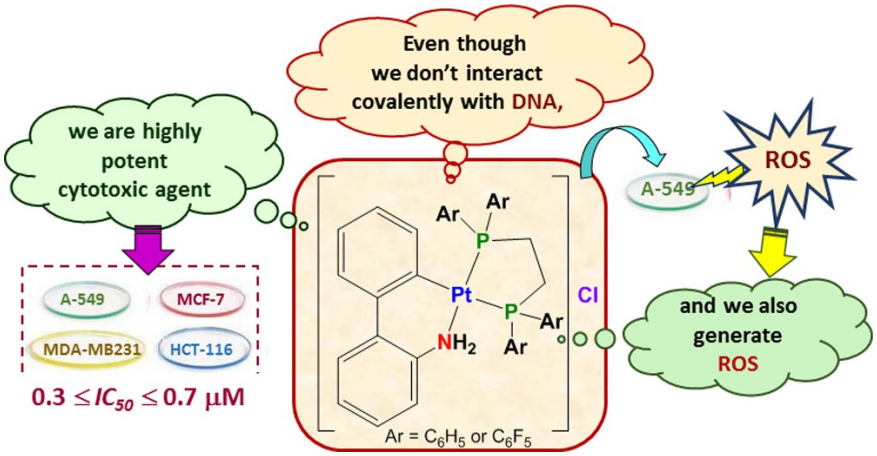

INTRODUCTION

Cisplatin is an efficient anticancer drug; in fact, it is the leading compound used against different types of cancer, such as ovarian, testicular, bladder, head, and neck cancers and small cell lung cancer. Nevertheless, this compound has a series of clinical disadvantages, with systemic toxicity being one of the main issues.1 The primary cisplatin target is DNA2 in both sick and healthy cells, without distinction. Furthermore, due to the affinity of platinum for some of the coordinating groups present in some biomolecules, cisplatin can interact and disrupt the functions of different proteins and enzymes, thus producing a variety of important side effects (only 1% of the intravenously administered drug actually reaches DNA). Furthermore, the efficiency of cisplatin is often lost after several chemotherapy cycles, since tumor cells become resistant.3 For these reasons, it is important to develop new anticancer agents with different coordination properties and mechanisms of action. Some of these mechanisms, among others, are DNA-binding with metallointercalators (π stacking interactions), mitochondria targeting (where mitochondrial DNA (mtDNA) damage can induce apoptosis without damaging nuclear DNA), and inhibition of some proteolytic enzymes such as cathepsin B (which is highly upregulated in a wide variety of cancers).4 Some coordination compounds offer the possibility of an alternative redox mechanism such as the generation of reactive oxygen species (ROS), an effective method of killing cancer cells.5 Furthermore, the induction of immunogenic cell death by chemotherapeutic platinum complexes6 and the use of a platinum(IV) prodrug targeting DNA damage repair7 have also been reported.

Cycloplatinated compounds have an increasing interest as anticancer agents,8 and compounds containing N-donor ligands9,10 have also been tested with very promising results. The high stability of these compounds may allow them to reach the cell unaltered. Furthermore, the presence of substitutionally active ligands favors covalent coordination to DNA, as for cisplatin, while the aromatic groups in the cyclometalated ligand might favor intercalative binding to DNA through π–π stacking.11 For these reasons, it seems interesting to study the use of compounds derived from the cycloplatination of 2-phenylaniline. This primary amine could afford an unusual six-membered platinacycle, which can modify the reactivity of the ligands in the coordination sphere and can be involved in hydrogen bonds through the NH2 group.

In spite of the continuous progress in the field of cyclometalation, the cycloplatination of primary amines remains relatively unexplored.12 The cycloplatination of substituted benzylamines has been reported by using a precursor obtained from K2[PtCl4] andHI13 or by reaction between the cis-[PtCl2(dmso)2], sodium acetate and the corresponding ligand.12b,14 It should be noted that in some of these cases there is an organic fragment in the α position of the coordinating atom which makes the cyclometalation reaction easier by decreasing the entropic requirements.15

To the best of our knowledge, there is a single report on the synthesis of six-membered metallacycles by cycloplatination of a primary amine. In an early work on the aqueous chemistry of mixed amines, cis-

and trans-platin analogues, Bednarsky et al. reported the cycloplatination of 1,2-bis(4-methoxyphenyl)-ethylamine and 2-(4-methoxyphenyl)-1-phenylethylamine and described that the metalation took place only on the methoxysubstituted ring.16

With these background in mind and following our studies on the synthesis and the applications of palladium and platinum metallacycles,10a,d,f,17 we describe here the cycloplatination of 2-phenylaniline and some preliminary biological studies to establish a structure−activity relationship of the cyclometalated platinum(II) complexes obtained to gain insight into its mechanisms of action. The cytotoxicity assessment of the new complexes was carried out on the moderate/highly resistant adenocarcinoma cells lines: A-549 lung, MDA-MB-231 and MCF-7 breast, and HCT-116 colon. Interactions with plasmid DNA (in presence or absence of topoisomerase I), inhibition of cathepsin B, cell cycle arrest, and induction of apoptosis were also studied. Moreover, herein, we address the question if the generation of reactive oxygen species (ROS) plays a role in the mechanisms of action of some of the synthesized compounds.

RESULTS AND DISCUSSION

Synthesis of the Cycloplatinated Compounds. The reaction of 2-phenylaniline with cis-[PtCl2(dmso)2] and sodium acetate in a 1/1/1 molar ratio in refluxing methanol for 24 h afforded cycloplatinated compound 2 in good yield. Methanol was selected as solvent because polar solvents favor the cyclometalation of primary amines.18 Shorter reaction times result in a rather low yield, and some metallic platinum is formed when longer times are used. If the reaction was carried out in the presence of proton sponge as an external base instead of sodium acetate, then no cycloplatinated compound was obtained, thus indicating that acetate acts as an internal base. All these results have been corroborated by a kinetico-mechanistic study of the cyclometalation reaction (see below).

As the presence of phosphines can increase the cytotoxic activity of platinum metallacycles19 the synthesis of 3−6 (two neutral and two ionic, more polar compounds) was also conducted, Scheme 1. Interestingly, compounds 3 and 4 have a relatively labile chlorido ligand in the coordination sphere, while in 5 or 6, vacant coordination positions are less facile, which should hinder their covalent interaction with DNA favouring other interaction mechanisms. We have selected two fluorinated derivatives 4 and 6 in order to explore the effects that fluorine atoms can induce on their bioactivity (the fluorous effect).20

New compounds 2−6 were characterized by elemental analyses and 1H, 31P-{1H}, 195Pt, and 19F NMR spectra. 1H NMR data are in agreement with the proposed structures. The aromatic proton in ortho position to the metal is coupled to platinum (3JH−Pt in the range 50−58 Hz). Coupling of the NH2 protons to platinum was only observed for compound 2 (2JH−Pt = 52 Hz); the signal width in compounds 3−6 preventing the determination of their 3JH−Pt. JP−Pt values obtained from 31P NMR spectra for 3 and 4 indicate that the phosphine ligand is trans to the amino group. For compounds 5 and 6, two resonances are observed in the 31P NMR spectrum with 1JP−Pt values of 1794 and 3828 Hz for 5 and 1712 and 4038 Hz for 6. The higher J value is assigned to the phosphorus atom trans to the amino, and the lower value is assigned to that trans to the metalated carbon in agreement with the higher trans influence of carbon atom.21 The 195Pt chemical shift values are in the expected range for cyclometalated platinum(II) compounds containing a phosphine and a chlorido ligand (compounds 3 and 4), as are those corresponding to cycloplatinated derivatives 5 and 6, containing two phosphorus donor atoms.

All the data agree with the structures proposed for neutral complexes 3 and 4 (in which the phosphine is in trans to the nitrogen atom) and the ionic structures of 5 and 6, in which there is one phosphorus atom trans to nitrogen and another phosphorus atom trans to the metalated carbon atom.19a

The 19F NMR spectrum of compound 4 displays one multiplet corresponding to the three equivalent para-fluoro substituents on the phosphine; in contrast, a much higher complexity is obtained for the spectrum of compound 6 in which three sets of four signals in the regions −122 to −128 ppm assigned to

166 8Fortho, −140 to −146 ppm assigned to 4Fpara, and −160 to −158 ppm assigned to 8Fmeta, are
167 observed. This fact shows the nonequivalence of the four pentafluorophenyl groups in the compound.22
168 Suitable crystals of 3 were obtained from a dichloromethanemethanol solution at room temperature and
169 were analyzed by X-ray diffraction (see Figure 1). This is the first known X-ray to 95.917(14)° for the
170 P(1)−Pt(1)−Cl(1) angle. The distances between platinum and the coordinated atoms are similar to those
171 reported for analogous compounds.23 The six-membered metallacycle presents a screw-boat
172 conformation with deviations from the mean plane of −0.394 Å for Pt(1), 0.538 Å for N(1), −0.184 Å
173 for C(1), −0.304 Å for C(2), 0.215 Å for C(3), and 0.129 Å for C(8). There are no π-stacking
174 interactions in the crystal, and an intermolecular interaction NH⋯Cl of 3.319 Å was observed.
175 **Kinetico-Mechanistic Study of the Metalation Reaction.** The kinetics of the reaction of cis-
176 [PtCl2(dmso)2] and 2-phenylaniline in the presence of NaAcO was studied in methanol solution at
177 different temperatures. Different [Pt]/[amine]/[NaAcO] concentration ratios were used to clarify the role
178 of the different species in the full process. The preliminary observation that the cyclometalation process
179 does not take place in the presence of proton sponge indicates that sodium acetate effectively acts as an
180 internal base, and that formation of acetate derivatives is a key step for the C−H bond activation
181 reaction.24,25 The fact that acetato derivative cis-[Pt(AcO)2(dmso)2] reacts in an equivalent manner as
182 checked by NMR confirms this assumption. Thus, the reaction seems to occur via an electrophilic
183 substitution mechanism in lieu of the standard oxidative addition processes occurring on Pt(II)
184 complexes,24,26 as already observed on similar acetato complexes of the same family.25
185 Careful time-resolved 1H NMR batch monitoring of the sequential set of processes occurring on mixing
186 methanol solutions of cis-[PtCl2(dmso)2] and 2-phenylaniline in the presence of NaAcO allowed to
187 discriminate the C−H bond activation reactions from the faster set of initial substitution processes. The
188 reaction rate constants of the metalation process at different temperatures, as determined by UV−vis
189 spectroscopy, produced the Eyring plot shown in Figure 2, from which the values structure of a six-
190 membered metallacycle containing a platinated primary amine. The platinum atom is in a square-planar
191 environment coordinated to carbon, chlorine, phosphorus and nitrogen. The phosphorus and nitrogen
192 atoms are in a trans arrangement. The angles between neighbor atoms in the coordination sphere lies in
193 the range of 84.09(4)° for N(1)−Pt(1)−Cl(1) the angle of ΔH# = 92 ± 5 kJ mol−1 and ΔS#=−45±15JK−1
194 mol−1 for the thermal activation parameters were derived. Interestingly the reaction rate constant is
195 found independent of the amount of NaAcO in the solution within the [Pt]/[NaAcO] = 0.5−3.0 margin,
196 neatly indicating that only the acetato derivatives, formed stoichiometrically at shorter times lead to the
197 C−H bond activation. On the contrary, the reaction rate constant slightly increases on increasing the
198 amount of free amine in solution (within the same [Pt]/[amine] = 0.5−3.0 margin). This fact indicates
199 that stoichiometric coordination of the primary amine does not take place readily, as observed in other
200 cases24,27 and that the initial substitution equilibrium reaction is also involved in the C−H activation
201 process.28,29 As a result the data collected in Figure 2 are specific for the [Pt] = [amine] = 5 × 10−4 M.
202 Even so, given the fact that the substitutional reactivity of the metal center is not expected to be rate-

203 limiting,26,30 the activation parameters derived should correspond to the proper C−H activation
204 process.
205 In this respect, the values derived for the thermal activation parameters indicate a process that is more
206 entropy driven than the only Pt(II) equivalent electrophilic substitution C−H bond activation reaction
207 studied from a kinetico-mechanistic perspective ($\Delta H\# = 76 \pm 5$ kJ mol−1 and $\Delta S\# = -101 \pm 16$ J K−1
208 mol−1).25 The formation of a relatively rigid six-membered metallacycle can be held responsible for the
209 difference, as observed for other systems with some flexibility constrains.31,32
210 **Biological Studies**. Platinum complexes are usually dissolved in dmso to conduct biologic experiments,
211 but it has been reported that on dissolving cisplatin in dmso a ligand displacement changes its structure
212 inhibiting its cytotoxicity and its ability to initiate cell death. For this reason it has been suggested that
213 new platinum drugs must demonstrate a lack of interaction with dmso.33
214 We carried out some experiments to evaluate the stability of the new platinum complexes in dmso and
215 dmso−water mixtures. We found that neutral compounds 3 and 4 containing a monodentate phosphine
216 are quite stable in dmso (3 days at room temperature), but when water is added to the dmso solution (a
217 30% solution, water−dmso), a little decomposition was observed by 31P NMR spectra. For instance, in
218 compound 3, new signals at 15.23 and 17.92 were observed. In contrast, ionic compounds 5 and 6 are
219 highly stable in dmso or dmso−water (1/1) solutions. After standing 3 days in deuterated dmso solution
220 plus 3 additional days in water−dmso (1/1), the 31P NMR spectra only show the expected two signals
221 plus the corresponding and typical platinum satellites (Figures S1 and S2). Furthermore, 1H and 31P
222 NMR spectrum also shows that 5 is stable in an aqueous biological media (phosphato buffer, pH 7.40),
223 showing that the cell culture medium does not change their chemical composition (Figures S3 and S4)
224 **Antiproliferative Assay.** The cytotoxicity of compounds 2−6 was evaluated in vitro against human
225 lung, breast, and colon cancer cell lines (A-549, MDA-MB-231 and MCF-7, and HCT-116,
226 respectively), using cisplatin as a positive control. Also, a normal human foreskin fibrobrast cell line
227 (BJ) was tested in the frame of the in vitro studies. The effects of the assayed platinacycles on the
228 growth of the selected cell lines were evaluated after 72 h, and the IC50 values (concentration at which
229 50% of cell growth is inhibited) are listed in Table 1. It can be seen that compounds 2−6 exhibit a high
230 antiproliferative activity in the four selected cell lines; however, very large differences in their cytotoxic
231 effectiveness are evident. Platinacycles 5 and 6 exhibited the lowest IC50 values within the series of the
232 moderate and highly resistant cancer cells lines tested (280−730 nM). For instance, 5 is approximately
233 33-fold more potent than cisplatin in A-549 lung cancer cells, 19- and 33-fold more potent in MDA-
234 MB-231 and MCF-7 breast cancer cells, respectively, and 70-fold more potent in the cisplatin-resistant
235 HCT-116 colon cancer cells. Interestingly, compounds 3−6 showed a lower antiproliferative activity in
236 normal BJ cells than that in the adenocarcinoma cell lines tested.
237 **DNA Interaction**. The interaction of 2−6 with DNA was assessed by their ability to modify the
238 electrophoretic mobility of the supercoiled closed circular (sc) form of pBluescript SK+ plasmid DNA.
239 Platinacycles 2, 3, and especially 4 alter the mobility of plasmid DNA (Figure 3). The coalescence point

240 for 4 is observed at 25 μM, while 2 and 3 show coalescence points at 50 μM. For the three compounds a
241 positive supercoiling was observed above the coalescence point concentrations. The electrophoretogram
242 of cisplatin shows a coalescence point at 10 μM and positive supercoiling above this concentration. On
243 the basis of the gel mobility shift assay, it is hypothesized that 2−4 alter the DNA tertiary structure by
244 the same mechanism as the standard reference, cisplatin but at higher concentrations. In contrast with
245 these findings, 5 and 6 were not effective at all for removing the supercoils of plasmid DNA. This
246 experiment shows the low reactivity related to substitution reactions of 5 and 6 when compared to
247 similar metallacycles19a pointing to a different mechanism of action or to an alternative biomolecular
248 target. It should be noted that some platinum-phosphato complexes have been shown to be cytotoxic in
249 ovarian cell lines yet they do not show any evidence of covalent binding to DNA.34
250 **Topoisomerase Inhibition.** In higher eukaryotes, DNA topoisomerases I are essential enzymes whose
251 main role is to relieve DNA supercoiling (torsional tension) ahead of replication and transcription
252 complexes. Nowadays, topoisomerase I is considered an important molecular target for anticancer drug
253 development. The efficient anticancer drug camptothecin, is a well-known topoisomerase I inhibitor.35
254 The anticancer activity of trinuclear (TriplatinNC, TriplatinNC-A),36 naphthoquinone Pt(II)
255 complexes,37 and luminescent cyclometalated Pt(II) compounds38 have been associated with their
256 ability to inhibit topoisomerase I.
257 A topoisomerase-based gel assay was performed to evaluate the ability of 5 and 6 to inhibit
258 topoisomerase I or to intercalate into DNA. The results given in Figure 4 show that 5 prevents
259 unwinding of DNA by the action of topoisomerase I, indicating that this compound is either intercalator
260 or topoisomerase I inhibitor. In contrast 6 did not prevent unwinding of DNA at concentrations below
261 100 μM.
262 To elucidate whether 5 is a DNA intercalator or a topoisomerase I inhibitor, relaxed pBluescript plasmid
263 DNA was incubated in the presence of topoisomerase I at increasing concentrations of compound 5. The
264 results are given in Figure 5 and show that 5 prevents winding of DNA by the action of topoisomerase I,
265 indicating that this compound is an inhibitor of topoisomerase I. This result agrees with the fact that the
266 nonplanarity of the six-membered metallacycle seems to exclude the possibility of DNA intercalation
267 (see X-ray structure of 3).
268 **Cathepsin B Inhibition.** Cathepsin B is a metalloprotease that in solid tumors has been proposed to
269 participate in metastasis, angiogenesis, and tumor progression. Recently, compounds based on
270 palladium, platinum, ruthenium, rhenium, gold, and tellurium were shown to be effective inhibitors of
271 cathepsin B.39 In addition, an excellent correlation between cathepsin B inhibition and cytotoxicity for
272 some dinuclear diphosphine palladacycles40 and mononuclear platinacycles containing a fluorinated
273 phosphine20 has been reported. Inhibition of cathepsin B has been also described for a
274 noncyclometalated trans-Pt(II) compound in our research group.19a We have determined the cathepsin
275 B inhibition activity for compounds 5 and 6. It should be noted that 5 inhibits cathepsin B (IC50 = 35 ±

276 4 μM), but 6, which presents a very similar chemical structure, did not show a significant cathepsin B
277 inhibition activity.
278 **Cell Cycle Dysregulation and Apoptosis Induction.**
279 Cell cycle dysregulation is considered to be one of the main hallmarks of cancer cells and proteins that
280 control the critical events of cell cycle have been proposed as useful antitumor targets.41 The effect of
281 compounds 3, 5, and 6 was evaluated on A-549 lung cancer cells. 3 and 6 play an important role in cell
282 cycle, while 5 does not affect it in a determinant manner. However, it is important to note that 3 and 6
283 have different modes of action since the former causes arrest mostly in S phase and the latter results in
284 an arrest in G1 phase (Figure 6).
285 As cancer is characterized by uncontrolled cellular proliferation, there is a considerable interest in
286 chemotherapeutic-induced apoptosis. The apoptosis-inducing properties of 3, 5, and 6 in A-549 cells
287 were examined by flow cytometry. Treating A-549 cells with 3 at its IC50 concentration (7 μM) for 72 h
288 resulted in ca. 10% decrease in the percentage of the cells alive, while the amount of early apoptotic
289 cells increased four times with respect to the control cells. The apoptosis induction potency of
290 compounds 5 and 6 showed great similarity to that of compound 3 (Figure 7). However, 3 and 5
291 increased the early apoptotic cell population, while 6 caused an increase in the population of late
292 apoptotic/necrotic cells. Hence the pathway that 3 and 5 follow for apoptosis induction seems to be
293 different from the apoptotic pathway of 6.
294 **Generation of Reactive Oxygen Species (ROS).** ROS are highly reactive oxygen metabolites that
295 include superoxide radicals (O2•−), hydrogen peroxide (H2O2), and hydroxyl radicals (OH•) among
296 others. ROS molecules participate in stress signaling and they are generated by several cellular
297 structures including mitochondria in all cells. Due to their increased proliferation rates, cancer cells need
298 to produce a large amount of ATP, which results in accumulation of ROS.42 Elevated ROS levels not
299 only activate intracellular signal transduction pathways that regulate multiple events in cancer but also
300 cause cancer cells to be more vulnerable to increased oxidative stress induced by exogenous ROS-
301 generating compounds. It has been shown that ROS may play an important role in cisplatin-induced
302 cytotoxicity and that glutathione (GSH) depletors increase this cytotoxicity by enhancing ROS
303 generation in bladder cancer cells.43
304 It has been recently described that the iridium(III) complex [Ir(5η-Cpxbiph)(Phpy)(py)]PF6 is a highly
305 cytotoxic compound and its mechanism of action is different from that is usual in platinum drugs. This
306 complex induces a significant increase in ROS levels in cancer cells. Chemical studies reveal that this
307 process involves catalytic hydride transfer from the coenzyme NADH to oxygen to produce H2O2 as a
308 ROS product.5a The amount of ROS produced by 3−6 was determined using DFCH-DA (2′,7′-
309 dichlorofluorescein diacetate) through FACS at their IC50 concentrations, after 24, 48, and 72 h of drug
310 exposure to the A-549 lung cancer cells.
311 Compounds 4−6 caused an enhancement in ROS levels after 24 h and a significant increase was
312 observed after 48 h of treatment for the tested A-549 tumor cell line (Figure 8). The increase in ROS

313 level was around 60% for 4, 40% for 5, and around 70% for 6 after treatment. Our results clearly
314 confirm that platinacycles 4−6 are able to increase ROS levels as part of their biological activities in
315 cancer cells and suggest that apoptosis induction observed in A-549 lung cancer cells treated with
316 compounds 5 and 6 might also be due to the increased ROS production since it is reported that increased
317 ROS can mediate the intrinsic mitochondrial apoptotic pathway.44 Interestingly, compound 3
318 significantly decreased the ROS levels at 24 h (around 50%) and 48 h (around 15%), while at 72 h, ROS
319 levels were naturalized. This result shows that 3 has antioxidant effect in short-term at A-549 cells and
320 that its cytotoxicity is not ROS dependent. There is a similar situation at Tarrado et al.45
321 Western blot analyses of proteins involved in cell cycle control and apoptosis were performed in order
322 to elucidate the mechanisms involved in the induction of apoptosis in A-549 cells due to the action of
323 compounds 3, 5, and 6. Incubation of A-549 cells with either their IC50 values or double their IC50 for
324 72 h resulted in activation of p53 tumor suppressor gene for 5
325 Activation of tumor suppressor p53 induces cell cycle arrest and apoptosis46 and considering that A-549
326 cells have wild type p53, this finding is concordant with the fact that the tested compounds are active in
327 apoptosis induction. In contrast, the increase in the active caspases 3 and 9 (24 h after the treatment)
328 indicates that 5 and 6 induce caspase dependent apoptosis in A-549 cells. Besides this, the inclusion of
329 caspase 9 shows that an intrinsic apoptotic stimuli is triggered by 5 and 6. Similarly, we observed an
330 increasing rate of Bax and a decreasing rate of Bcl-2 after 24 h of treating cells with test compounds.
331 Taking into account that Bax is a pro-apoptotic protein and Bcl-2 is an antiapoptotic protein, we can
332 deduce that all three compounds lead cells to apoptosis induction. It has been reported that ROS down-
333 regulates Bcl-2 protein, in agreement with the idea that the induced apoptosis is mediated by increased
334 ROS level owing to the action of 5 and 6.
335 The increase in ROS levels in A-549 lung cancer cells induced by complexes 5 and 6 prompted us to
336 study the reaction of these compounds with potential cellular reducing agents, following the
337 experimental procedure previously described.5a It is well-known that coenzyme NADH plays an
338 important role in several biocatalyzed processes and NADH/NAD+ is an important redox couple which
339 maintains the redox balance in cells. To show whether reaction of platinacycles 5 and 6 with NADH
340 could produce ROS, experiments of 1H NMR and UV/vis spectroscopy were carried out. The addition
341 of NADH (3.5 mol equiv) to a 0.8 mM solution of complex 6 leads to new signals in proton NMR at
342 aprox. 9.25, 9.50, and 9.75 ppm, corresponding to the hydrogen atoms at the C-4, C-6, and C-2 positions
343 respectively of the nicotinamide ring of the newly formed NAD+ (Figure S5). Oxidation of NADH to
344 NAD+ was also observed with 1/5 and even 1/10 dilution of compound 6. UV/vis spectroscopy studies
345 were carried out to quantify the magnitude of this catalytic mechanism. Interestingly the data from the
346 UV/vis spectroscopy assay showed that platinacycles 5 and 6 may act as catalysts for hydride transfer
347 from NADH with a turnover number (TON) of ca. 5 and 17, respectively. The formation of NAD+ was
348 confirmed by a decrease in intensity of the characteristic NADH band at 341 nm and the simultaneous
349 increase in intensity at 260 nm. The results for 6 are depicted in Figure S6, and the concentration of

reacted NADH was calculated by measuring the absorption difference at 341 nm, taking into account the extinction coefficient of NADH (ε = 6220 $M^{-1}cm^{-1}$). These results are in agreement with the lower ROS generation increase observed for compound 5 by FACS in comparison with compound 6 in A-549 lung cancer cells. However, the formation of H_2O_2 was observed when NADH (3 mol equiv) was added to a solution of complex 6 (1 mM) in a mixture of MeOH/H_2O (3:7) using H_2O_2 test stick (Figure S7). The observed blue color matches with a concentration of approximately 0.2 mM of H_2O_2. The results obtained by 1H NMR and UV/vis spectroscopies and the H_2O_2 test stick clearly demonstrate the production of ROS and indicate that the oxidant anticancer activity previously reported for hexacoordinated iridium(III) compounds5a can also be extrapolated to some platinum(II) square-planar complexes.

DFT Calculations. We have carried out some DFT theoretical calculations in order to assess the distinct behaviour observed between complexes with monodentate and bidentate phosphines. The ability of iridium complexes to act as ROS generators has been proved to depend on the ability of the metal atom to accept a hydride ion from NADH.47 Thus, we have explored the reaction of the platinum(II) complexes to form hydrides. We have used MNH (N-methyl-1,4-dihydronicotinamide) as a model for NADH, and the results obtained are summarized in Scheme S1.

Our results suggest that the most energetically favorable path to form an hydrido complex begins with the substitution of the ligand trans to the metalated carbon by water, in agreement with the higher trans influence of the carbon atom.21 The substitution of a chloride ligand by water in the complexes with monodentate phosphines is exoergic. In contrast, this first step is strongly disfavored for 5 and 6 in which one of the phosphorus atoms of the diphosphine ligand should be substituted by water. This fact explains the great stability of 5 and 6 in cell culture medium and the fact that they do not show covalent interaction with DNA.

The second step that we have considered is the reaction of the aqua complexes with MNH to form the hydride complex and MN^+. This reaction is endoergic, with ΔE following the sequence 6 < 4 < 3 < 5. However, our results indicate that the complexes with chelating diphosphine lignads result in a more favorable path: substitution of the diphosphine for a second water ligand followed by the proper reaction with MNH, resulting in the formation of an hydrido ligand trans to the nitrogen atom, in agreement with the transphobia effect.48 This path is strongly disfavored for the complexes with monodentate phosphines.

When this second path is considered for 5 and 6, the energy variations corresponding to the global reaction are −62.3, 42.7, and 49.4 kJ/mol for 6, 4, and 5 respectively, in agreement with their respective ROS abilities. Scheme 2 shows a plausible mechanism for the platinum(II) catalytic generation of hydrogen peroxide, which is similar to the proposal for Ir(III) complexes.5a

CONCLUSIONS

Six-membered nonplanar platinacycles, containing bidentate phosphines, show high cytotoxicity despite not exhibiting covalent interaction with DNA. Despite 5 and 6 having very similar chemical structures, distinct bioactivity has been found. The presence of perfluoroaromatic rings in 6 hinders its interaction with some proteins. This is an interesting issue given that the side effects of cisplatin have been related with the high affinity of the platinum for the coordinating atoms present in some biomolecules. It has been shown that 6 induces an increase of the ROS levels in the nonmicrocytic A-549 lung cancer cells, and interestingly, this compound is also able to oxidize NADH by a catalytic process to produce ROS H2O2. The Western blot analyses of proteins involved in cell cycle control and apoptosis in A-549 cells revealed intrinsic apoptotic stimuli, and that the induced apoptosis is mediated by an increased ROS level. It seems that the use of platinum(II) compounds containing chelated polyfluorated ligands might be an interesting strategy in order to get highly effective anticancer drugs, able to modulate redox pathways in cisplatin resistant cancer cells, minimizing secondary side effects.

EXPERIMENTAL SECTION

All chemicals were obtained from commercial sources and used as received. Solvents were distilled and dried before use,49 cis-[PtCl2(dmso)2] and cis-[Pt(AcO)2(dmso)2] were prepared using reported procedures.50,51

NMR Labeling.

Preparation of the Compounds. [PtCl{κ2-N2′,C1-2-(2′-NH2C6H4)-C6H4}(dmso)] (2). A mixture of 300 mg (0.71 mmol) of cis-[PtCl2dmso)2], 120 mg (0.71 mmol) of 2-aminobiphenyl, and 58 mg (0.71 mmol) of sodium acetate in 20 mL of methanol was refluxed for 24 h. The resulting solution was filtered, the solvent evaporated, and the residue recrystallized from CH2Cl2−diethyleter to obtain 2 as a white solid. Yield: 210 mg (60%). 1H NMR (400 MHz, CDCl3), δ = 7.68 (d, JPtH = 52, 3JH−H = 6.0, 1H, Ha), 7.51 (d, 3JH−H = 7.60, 1H), 7.34 (d, 3JH−H = 8.0, 1H), 7.27 (t, 3JH−H = 7.60, 1H), 7.21−7.06 (m, 4H), 5.50 (s, JPt−H = 52, 2H, NH2), 3.30 (s, 6H, dmso). 195Pt NMR (85.68 MHz, CDCl3), δ = −3817.1 (s). EA (calc. for C14H16ClNOPtS): C: 34.8% (35.26%); H: 3.6% (3.38%); N: 2.8% (2.94%); S: 6.8 (6.72%). MS-ESI+: m/z = 441.0 (calcd: 441.06) [M − Cl + CH3CN]+.

[PtCl{κ2-N2′,C1-2-(2′-NH2C6H4)C6H4}{P(C6H5)3}] (3). Compound 3 was obtained after stirring at room temperature for 4 h a solution containing 300 mg (0.63 mmol) of compound 2 and 200 mg (0.63 mmol) of PPh3 in 20 mL of acetone. The resulting solution was filtered, the solvent evaporated, and the residue treated with diethyleter. The pale yellow solid obtained was filtered and dried in vacuum. Yield: 410 mg (90%). 1H NMR (400 MHz, dmso-d6), δ = 7.70 (br, 2H, NH2). 7.60−7.20 (m, 20H), 6.82 (t, 3JH−H = 7.4, 1H, Hc), 6.55 (d 3JH−H = 7.4, 1H, Ha), 6.26 (t, 3JH−H = 7.5, 1H, Hb). 31P NMR (161.98 MHz, dmso-d6), δ = 16.49 (s, 1JP−Pt = 4541.9). 195Pt NMR (85.68 MHz, dmso-d6), δ = −4098,1 (d, 1JP−Pt = 4541.9). EA (calcd for C30H25ClNPPt): C: 54.7% (54.51%); H: 3.9% (3.81%) and N: 1.9% (2.12%). MS-ESI+: m/z = 625.1, (calcd: 625.13) [M − Cl]+.

[PtCl{κ2-N2′,C1-2-(2′-NH2C6H4)C6H4}{P(4-FC6H4)3}] (4). Compound 4 was obtained after stirring at room temperature for 2 h a solution containing 200 mg (0.420 mmol) of compound 2 and 132.8 mg (0.420 mmol) of P(4-FC6H4)3 in 20 mL of acetone. The white solid formed was filtered off and discarded. The solvent was evaporated, the residue treated with CH2Cl2 (5 mL) and methanol (5 mL), and the obtained mixture kept at low temperature overnight. The whitish solid obtained was filtered and dried in vacuum. Yield: 81 mg (27%). 1HNMR (400 MHz, CDCl3), δ = 7.50 (dd, JH−H = 7.6; 1.2, 1H), 7.44 (ddd, JH−H/F = 11.2, 8.8, 5.2, 6H, PR3), 7.24 (td, JH−H = 7.6, 1.6, 1H), 7.21 (dd, JH−H = 8.0, 1.6, 1H), 7.18−7.13 (m, 2H), 6.92 (td, JH−H/F = 8.8, 2.0, 6H, PR3), 6.85 (td, JH−H = 7.6, 1.2, 1H, Hc), 6.45 (ddd, JH−H = 7.6, 2.4, 1.2, 3JH−Pt = 56.0, 1H, Ha), 6.36 (td, JH−H = 7.6, 1.2, 1H, Hb), 5.38 (s, br, 2H, NH2).19F NMR (376.45 MHz, CDCl3), δ = −108.6 (m). 31P NMR (161.98 MHz, CDCl3), δ = 14.36 (s, 1JP−Pt = 4568.0). 195Pt NMR (85.68 MHz, CDCl3), δ = −4099,6 (d, 1JP−Pt = 4594.3). EA (calcd for C30H22ClF3NPPt): C: 51.3% (50.39%); H: 3.4% (3.10%); N: 1.8% (1.96%). MS-ESI+: m/z = 679.1, (calcd: 679.11) [M − Cl]+.

[Pt{κ2-N2′,C1-2-(2′-NH2C6H4)C6H4}(C6H5)2PCH2CH2P(C6H5)2}]Cl (5). Compound 5 was obtained after stirring at room temperature for 2 h a solution containing 275 mg (0.54 mmol) of compound 2 and 214 mg (0.54 mmol) of (C6H5)2PCH2CH2P(C6H5)2 in 20 mL of acetone. The white solid formed was filtered off and discarded, the solvent evaporated, and the residue recrystallized from CH2Cl2−diethyleter to obtain 5. Yield: 150 mg (35%). 1H NMR (500 MHz, CDCl3, 220 K), δ = 8.15 (br, 2H,NH2), 7.70−7.25 (br m, 22H), 7.15 (t, 3JH−H = 7.5, 1H), 7.03 (t, 3JH−H = 7.5, 1H), 6.77 (t, 3JH−H = 7.5, 1H), 6.64 (t, 3JH−H = 7.5, 1H), 6.25 (d, 3JH−H = 7.5, 1H), 6.18 (t, 3JH−H = 7.5, 1H), 2.90−2.50 (br, 2H, CH2P); 2.25−2.05 (br, 2H, CH2P). 31P NMR (161.98 MHz, CDCl3), δ = 45.4 (s, 1JP−Pt = 1794.1 PA), 39.8 (s, 1JP−Pt = 3827.9, PB). EA (calcd for C38H34ClNP2Pt): C: 57.0% (57.25%); H: 4.6% (4.30%); N: 1.6% (1.76%). MS-ESI+: m/z = 761.2, (calcd: 761.18) [M − Cl]+.

[Pt{κ2-N2′,C1-2-(2′-NH2C6H4)C6H4}(C6F5)2PCH2CH2P(C6F5)2}]Cl (6). Compound 6 was obtained after stirring at room temperature for 2 h a solution containing 133 mg (0.279 mmol) of compound 2 and 212 mg (0.279 mmol) of (C6F5)2PCH2CH2P(C6F5)2 in 20 mL of acetone. The white solid formed was filtered off and discarded, the solvent evaporated, and the residue treated with diethyl ether. The white solid obtained was filtered and dried in vacuum. Yield: 204 mg (63%). 1H NMR (400 MHz, dmso-d6), δ = 8.60 (s, br, 2H, NH2), 7.42 (m, 2H), 7.25 (m, 2H), 7.08 (t, JH−H = 7.6, 1H), 7.03 (t, JH−H = 7.5, 1H), 6.89 (t, JH−H = 7.7, 1H), 6.47 (d, JH−H = 7.7, 1H), 3.50 (br, 1H); 3.15 (br, 1H); 2.85 (br, 2H). 19F NMR (376.45 MHz, dmso-d6), δ = −122.16 (s, br, 2F, Fo), −125.66 (s, br, 2F, Fo), −127.12 (s, br, 2F, Fo), −127.30 (s, br, 2F, Fo), −140.59 (s, br, 1F, Fp), −142.44 (s, br, 1F, Fp), −143.47 (s, br, 1F, Fp), −145.18 (s, br, 1F, Fp), −156.03 (s, br, 2F, Fm), −157.63 (s, br, 2F, Fm), −157.67 (s, br, 2F, Fm), −158.02 (t, 2JF−F = 18.8, 2F, Fm). 31P NMR (161.98 MHz, dmso-d6), δ = 8.10 (d, 1JP−Pt = 1712.1, 2JP A –P B = 24.3, PA), 1.98 (d, 1JP−Pt = 4073.8, 2JP A –P B = 24.3, PB). 195Pt NMR (85.68 MHz, dmso-d6), δ = −4399.5(dd, 1JP A −Pt = 4054.5, 1JP B −Pt = 1691.0). EA (calcd for C38H14ClF20NP2Pt): C: 39.2% (39.45%); H: 1.4% (1.22%); N: 1.2% (1.21%). MS-ESI+: m/z = 1121.0, (calcd: 1120.99) [M − Cl]+.

METHODS AND INSTRUMENTATION

Elemental Analysis. C, H, and N analyses were performed with an Eager 1108 microanalyzer.

NMR Spectroscppy. NMR spectra were recorded in CDCl3 at 298 K with Mercury 400 (1H, 19F) and Bruker 400 Avance III HD (31P, 195Pt) spectrometers. Chemical shifts are given in δ values (ppm) relative to SiMe4 (1H), 85% H3PO4 (31P{1H}), CF3Cl (19F), and H2PtCl6 in D2O (195Pt), and coupling constants are given in Hz. Multiplicity is expressed as s (singlet), d (doublet), t (triplet), and m (multiplet).

Electrospray Ionization Mass Spectrometry. Low-resolution ESI (+) spectra were acquired either on an LC/MSD-TOF instrument or on a ZQ mass spectrometer, utilizing a mixture of H2O/CH3CN (1:1, v/v) as the eluent.

Crystal Data and Structure Refinement for 3. A yellow prismlike specimen of C30H25ClNPPt, approximate dimensions 0.124 mm × 0.148 mm × 0.595 mm was used for the X-ray crystallographic analysis. The X-ray intensity data were measured on a D8 Venture system equipped with a multilayer monochromator and a Mo microfocus (λ = 0.71073 Å).

The frames were integrated with the Bruker SAINT software package using a narrow-frame algorithm. The integration of the data using a triclinic unit cell yielded a total of 62233 reflections to a maximum θ angle of 30.55° (0.70 Å resolution), of which 7525 were independent (average redundancy 8.270, completeness = 99.9%, Rint = 2.76%, Rsig = 1.37%) and 7380 (98.07%) were greater than 2σ(F2). The final cell constants of a = 9.7646(4) Å, b = 10.0995(4) Å, c = 12.4955(6) Å, α = 92.0540(10)°, β = 92.224(2)°, γ = 93.7040(10)°, volume = 1227.87(9) Å3, are based upon the refinement of the XYZcentroids of reflections above 2θ σ(I). Data were corrected for absorption effects using the multiscan method (SADABS). The calculated minimum and maximum transmission coefficients (based on crystal size) are 0.5526 and 0.7461. The structure was solved using the Bruker SHELXTL Software Package, and refined using SHELXL,52 using the space group $P\bar{1}$, with Z = 2 for the formula unit, C30H25ClNPPt. The final anisotropic full-matrix least-squares refinement on F2 with 313 variables converged at R1 = 1.54%, for the observed data and wR2 = 4.10% for all data. The goodness-of-fit was 1.281. The largest peak in the final difference electron density synthesis was 0.808 e− Å−3 and the largest hole was −1.986 e− Å−3 with an RMS deviation of 0.173 e− Å−3. On the basis of the final model, the calculated density was 1.788 g cm−3 and F(000) 644 e−. Further details concerning the resolution and refinement of these crystal structures are given in Table S1.

Kinetics. The reactions were followed by UV−vis spectroscopy in the 600−300 nm range on an HP8453 or Cary−50 instruments equipped with a thermostated multicell transport. Rate constants were derived from absorbance versus time traces at the wavelengths where a maximum increase and/or decrease of absorbance was observed. The values of k were derived by the standard SPECFIT o REACTLAB software;53,54 no dependence of the observed rate constant values on the selected wavelengths was detected. The general kinetic technique is that previously described55 and involved mixing stock

methanol solutions of the reactants to achieve the final desired concentrations in the UV−vis cell being monitored. Rate constants calculation was conducted on the initial 3t1/2 of the reaction with a platinum complex concentration of 5 × 10−4 M and varying the concentrations of amine and acetate as indicated in the text.

Cell Culture. Human lung adenocarcinoma cells, A-549, and human breast adenocarcinoma cells, MDA-MB-231, were grown as a monolayer culture in Dubecco's modified Eagle's medium (DMEM) with L-glutamine, without glucose and without sodium pyruvate) in the presence of 10% heat-inactivated fetal bovine serum (FBS), 10 mM D-glucose, 2 mM L-glutamine, and 0.1% streptomycin/penicillin. The other human breast adenocarcinoma cell line, MCF-7, was cultured in minimum essential medium (MEM without phenol red), containing 10% fetal bovine serum (FBS), 10 mM D-glucose, 1 mM sodium pyruvate, 2 mM L-glutamine, 0.1% streptomycin/penicillin, 0.01 mg/mL insulin, and 1% nonessential amino acids. Human colorectal carcinoma cells, HCT-116, were cultured in DMEM/HAM F12 (1:1 volume) mixture containing 10% FBS, 4 mM L-glutamine, 12.5 mM D-glucose, and 0.1% streptomycin/penicillin. Human skin fibroblast cell line, BJ, was cultured in DMEM in the presence of 10% FBS, 12.5 mM D-glucose, 4 mM L-glutamine, 5 mM pyruvate, and 0.5% streptomycin/ penicillin. All the cells were incubated in standard culture conditions (humidified air with 5% CO2 at 37 °C).

Cell Viability Assay. To assess the viability assays of all the cell lines, the platinum compounds were suspended in high purity DMSO at a final concentration of 20 mM as stock solution. To obtain final assay concentrations, they were diluted in the corresponding culture medium (final concentration of DMSO was the same for all conditions, and was always lower than 1%). In the case of cisplatin, a stock solution in water of cisplatin (1 mg/mL) was diluted with water until final assay concentrations. The assay was performed by a variation of the MTT (3-(4,5-dimethylthiazol-2-yl)-2,5-diphenyltetrazolium bromide) assay,56,57 which is based on the ability of alive cells to cleave the tetrazolium ring of the MTT thus producing formazan, which absorbs the light at 550 nm. In brief, the corresponding number of cells per well (2.5 × 103 A-549 cells/well, 1 × 104 MDA-MB-231 cells/well, 1 × 104 MCF-7 cells/well, 1.5 × 103 HCT-116 cells/well, and 1 × 104 BJ cells/well) were cultured in 96-well plates for 24 h prior to the addition of different compounds at different concentrations, in triplicates. After incubation for 72 h with compounds, the media was aspirated and 100 μL of filtered MTT (0.5 mg/mL) were added to each well. Following 1 h of incubation with the MTT, the supernatant was removed, and the precipitated formazan was dissolved in 100 μL of DMSO. Relative cell viability, compared to the viability of untreated cells, was measured by absorbance at 550 nm on an ELISA plate reader (Tecan Sunrise MR20−301, TECAN, Salzburg, Austria). Concentrations that inhibited cell growth by 50% (IC50) after 72 h of treatment were subsequently calculated.

DNA Migration Studies. A stock solution (10 mM) of each compound was prepared in high-purity DMSO. Then, serial dilutions were made in Milli-Q water (1:1). Plasmid pBluescript SK+ (Stratagene) was obtained using QIAGEN plasmid midi kit as described by the manufacturer. Interaction of drugs

537 with pBluescript SK+ plasmid DNA was analyzed by agarose gel electrophoresis.58 Plasmid DNA
538 aliquots (40 μg/mL) were incubated in TE buffer (10 mM Tris-HCl, 1 mM EDTA, pH 7.5) with
539 different concentrations of compounds 2−6 ranging from 0 to 200 μM at 37 °C for 24 h. Final DMSO
540 concentration in the reactions was always lower than 1%. For comparison, cisplatin, and EB were used
541 as reference controls. Aliquots of 20 μL of the incubated solutions containing 0.8 μg of DNA were
542 subjected to 1% agarose gel electrophoresis in TAE buffer (40 mM tris-acetate, 2 mM EDTA, pH 8.0).
543 The gel was stained in TAE buffer containing EB (0.5 mg/mL) and visualized and photographed under
544 UV light.
545 **Topoisomerase I Inhibition**. Topoisomerase I-based experiments were performed as described
546 previously.59 Supercoiled pBluescript DNA, obtained as described above, was treated with
547 topoisomerase I in the absence or presence of increasing concentrations of compounds 5 and 6. Assay
548 mixtures contained supercoiled pBluescript DNA (0.8 μg), calf thymus topoisomerase I (3 units) and
549 complexes 5 and 6 (0−100 μM) in 20 μL of relaxation buffer Tris-HCl buffer (pH 7.5) containing 175
550 mM KCl, 5 mM MgCl2, and 0.1 mM EDTA. EB (10 μM) was used as a control of intercalating agents,
551 and etoposide (E, 100 μM) was a control of nonintercalating agent. Reactions were incubated for 30 min
552 at 37 °C and stopped by the addition of 2 μL of agarose gel loading buffer. Samples were then subjected
553 to electrophoresis and DNA bands stained with ethidium bromide as described above.
554 To distinguish whether compounds act as topoisomerase inhibitors or DNA intercalators, the conversion
555 of relaxed DNA to a supercoiled state caused by the compounds was analyzed in the presence of
556 topoisomerase I. Relaxed DNA was obtained by incubation of supercoiled DNA with topoisomerase I as
557 described above. Assay mixtures (20 μL) contained: relaxed DNA, topisomerase I (3 units), and
558 compound (50 μM or 100 μM). Reactions were incubated 20 min at 37 °C and stopped as described
559 above. EB (10 μM) was used as a control of intercalative drug.
560 **Cathepsin B Inhibition Assay.** The colorimetric cathepsin B assay was performed as described by
561 Casini et al.60 with few modifications. Briefly, the reaction mixture contained 100 mM sodium
562 phosphate (pH 6.0), 1 mM EDTA, and 200 μM sodium N-carbobenzoxy-Llysine p-nitrophenyl ester as
563 substrate. To have the enzyme catalytically active before each experiment, the cysteine in the active site
564 was reduced by treatment with dithiothreitol (DTT). For this purpose, 5 mM DTT was added to
565 cathepsin B sample before dilution and incubated 1 h at 30 °C. To test the inhibitory effect of the
566 platinum compounds on cathepsin B, activity measurements were performed in triplicate using fixed
567 concentrations of enzyme (1 μM) and substrate (200 μM). The platinum compounds were used at
568 concentrations ranging from 5 to 100 μM. Previous to the addition of substrate, cathepsin B was
569 incubated with the different compounds at 25 °C for 2 h. The cysteine proteinase inhibitor E-64 was
570 used as a positive control of cathepsin B inhibition. Complete inhibition was achieved at 10 μM
571 concentration of E-64. Activity was measured over 90 s at 326 nm on a UV spectrophotometer.
572 **Cell Cycle Analysis**. Cell cycle was assessed by flow cytometry using a fluorescence activated cell
573 sorter (FACS). For this assay, 5×104 A-549 cells were seeded in 6 well plates with 2 mL of medium.

After 24 h of incubation, 3, 5, and 6 were added at their IC50 values (7.0, 0.28, and 0.73 μM, respectively). Following 72 h of incubation, cells were harvested by mild tripsinization, collected by centrifugation and resuspended in Tris-buffered saline (TBS) containing 50 mg/mL PI, 10 mg/mL DNase-free RNase, and 0.1% Igepal CA-630. The cell suspension was incubated for 1 h at room temperature to allow for the staining of the cells with the PI, and afterward, FACS analysis was carried out at 488 nm in an Epics XL flow cytometer (Coulter Corporation, Hialeah, FL). Data from 1 × 104 cells were collected and analyzed using the Multicycle program (Phoenix Flow Systems, San Diego, CA).

Apoptosis Assay. Apoptosis was assessed evaluating the annexin-V binding to phosphatidylserine (PS), which is externalized early in the apoptotic process. First, 5 ×104 A-549 cells per well were seeded in 6-well plates with 2 mL of medium and treated as described above for the cell cycle analysis assay. After cell collection and centrifugation, cells were resuspended in 95 μL binding buffer (10 mM HEPES/NaOH, pH 7.4, 140 mM NaCl, 2.5 mM CaCl2). Then, 3 μL of Annexin-V FITC conjugate (1 mg/mL) was then added, and the suspension was incubated in darkness for 30 min, at room temperature. Just before FACS analysis, the cell suspension was added to a vial containing 500 μL of binding buffer, and then stained with 20 μL of 1 mg/mL PI solution. Data from 1 × 104 cells were collected and analyzed.

Data Analysis. For each compound, a minimum of three independent experiments with triplicate values to measure antiproliferative activity and a minimum of two independent experiments for cell cycle analysis and assessment of apoptosis were conducted. Data are given as the mean ± standard deviation (SD).

Determination of Intracellular Reactive Oxygen Species (ROS) Levels. A-549 lung cancer cells were grown on 6-well plates to 70% confluence, washed once with warm PBS, and incubated with 5 μM 2′-7′-dichlorofluorescein diacetate (DCFH-DA, Invitrogen) in PBS supplemented with 5.5 mM glucose and 2 mM glutamine. After incubation at 37 °C for 30 min, PBS was replaced with complete culture medium, and the cells were incubated for another 50 min at 37 °C. Finally, cells were trypsinized and resuspended thoroughly with 0.4 mL of PBS, DCFH-DA (50 μM), and PI(20 μg/mL). Intracellular internalized probe reacts with ROS and emits fluorescence when excited at 492 nm. Emitted fluorescence was recorded by flow cytometry at 520 nm using an Epics XL flow cytometer (Coulter Corporation, Hialeah, FL, USA). Data of DCF fluorescence concentrations from 1 × 104 PI negative cells were collected and analyzed using multicycle program (Phoenix FlowSystems, San Diego, CA, USA)·45

Western Blot Analysis. For this assay, 5 × 104 A-549 cells were seeded in 6-well plates with 2 mL of medium. After 24 h of incubation, 3, 5, and 6 were added at their IC50 values or double of IC50 values (7.0, 0.28, and 0.73 μM, or 14, 0.56, and 1.46 μM respectively). Following 24, 48, or 72 h of incubation, whole cell lysate containing total protein extract was isolated by using RIPA buffer containing 50 mM Tris (pH 8.0), 150 mM sodium chloride, 1% Triton X-100, 0.5% sodium deoxycholate, 0.1% sodium

611 dodecyl sulfate (SDS), 1% protease inhibitor cocktail (Thermo Fisher Scientific Inc.), and 1%
612 phosphatase cocktail (Thermo Fisher Scientific Inc.). Cells were scraped, sonicated and centrifuged at
613 15 000 g for 20 min at 4 °C. Supernatants were recovered, and protein content was quantified by the
614 BCA kit (Pierce Biotechnology). Then, 20 mg of protein was loaded on a 10% SDS-polyacrylamide gel
615 and transferred to a polyvinyl nitrocellulose transfer membrane (Bio-Rad Laboratories). The membranes
616 were blocked by incubation at room temperature in PBS buffer containing 0.1% of Tween and 5% dry
617 milk for 1 h and washed three times with PBS−0.1% Tween. Then, membranes were blotted with the
618 primary antibodies overnight at 4 °C. After primary antibody incubation, the blots were washed three
619 times with PBS−0.1% Tween and incubated with the appropriate secondary antibody for 1 h at room
620 temperature. After secondary antibody incubation, membranes were washed again three times with
621 TBS−0.1% Tween before protein detection. All blots were treated with the Immobilon ECL Western
622 Blotting Detection Kit Reagent (Millipore) and developed after exposure to an autoradiography film in a
623 film cassette. The primary antibodies used were Bax (Santa Cruz Biotechnology), Bcl-2 (Santa Cruz
624 Biotechnology), caspase 3 and 9 (Cell Signaling Technology), cleaved caspase 3 (Cell Signaling
625 Technology), p53 (Calbiochem), PARP (Pharmingen), and β-actin (MP Biomedicals).
626 **Interactions of 6 with NADH.** NADH (3.5 mol equiv) was added to an NMR tube containing a 0.8 mM
627 solution of complex 6 in 50% methanol-d4 50% D2O at ambient temperature. 1H NMR spectra of the
628 resulting solution was recorded at 310 K at 0 and 72 h and 1 week.
629 **UV/Vis Detected Catalytic Reaction of Compound 6 with NADH**. Reaction between 6 (0.8 μM) with
630 NADH (87 μM) in H2O was monitored by UV−vis at 310 K for 22 h. In order to dissolve compound 6,
631 a few drops of MeOH were used. Turnover number (TON) is defined as the number of moles of NADH
632 that a mole of catalyst (compound 6) can convert within 22 h. TON was calculated from the difference
633 in NADH concentration after 22 h divided by the concentration of compound 6 (catalyst). The
634 concentration of NADH was obtained using the extinction coefficient ε339 = 6220 M−1cm−1.
635 **Detection of H2O2**. For the reaction of compound 6 (1 mM) with 3 mol equiv NADH in 30%
636 MeOH/70% H2O (v/v) at 310 K, H2O2 was detected by quantofix peroxide test sticks (Peroxid 25 from
637 Sigma-Aldrich).
638 **Theoretical Calculations.** Each system has been studied using the following procedure: First, the most
639 stable conformation has been determined using molecular mechanics, with the Spartan '14 software;61
640 the MMFF force field62 has been chosen. Geometries and energies have been calculated at the DFT
641 level, using the B3LYP functional63 as implemented in Gaussian 03.64 The basis set has been chosen as
642 follows: LANL2DZ65 for Pt and 6-31G*,66 including polarization functions for non-hydrogen atoms,
643 for H, C, N, O, P, and F. Solvation effects have been calculated using the CPCM method.67
644

AUTHOR INFORMATION

Corresponding Authors

*E-mail: jaumegranell@qi.ub.es.

*E-mail: quirantese@ub.edu.

ORCID

Margarita Crespo: 0000-0002-7086-9751

Jaume Granell: 0000-0001-6360-7043

Notes

The authors declare no competing financial interest.

ACKNOWLEDGEMENTS

We thank the Ministerio de Economía y Competitividad (grant numbers CTQ2015 65040-P, CTQ2015-65707-C2-1-P MINECO/ FEDER, SAF2017-89673-R, CTQ2017-90802-REDT), Generalitat de Catalunya (2017SGR1033 and 2014SGR0155), the Instituto de Salud Carlos III and Centro de Investigación Biomédica en Red de Enfermedades Hepáticas y Digestivas (CIBERHD, CB17/04/00023), and Icrea Academia award 2010 (M. Cascante) for financial support, and Dr. Francisco Cardenas for the NMR studies. Dedicated to Prof. Ernesto Carmona on the occasion of his retirement in appreciation of his outstanding contributions to organometallic chemistry.

667 **REFERENCES**

668

669 (1) Medici, S.; Peana, M.; Nurchi, V. M.; Lachowicz, J. I.; Crisponi, G.; Zoroddu, M. A. Coord.
670 Chem. Rev. 2015, 284, 329−350.

671 (2) (a) Roberts, J. J.; Thomson, A. J. Prog. Nucleic Acid Res. Mol. Biol. 1979, 22, 71−133. (b)
672 Lippard, S. J. Science 1982, 218, 1075−1082.

673 (3) (a) Wilson, J. J.; Lippard, S. J. Chem. Rev. 2014, 114, 4470−4495. (b) Shen, D. W.; Pouliot, L.
674 M.; Hall, M. D.; Gottesman, M. M. Pharmacol. Rev. 2012, 64, 706−721.

675 (4) (a) Johnstone, T. C.; Suntharalingam, K.; Lippard, S. J. Chem. Rev. 2016, 116, 3436−3486. (b)
676 Allardyce, C. S.; Dyson, P. J. Dalton Trans. 2016, 45, 3201−3209.

677 (5) (a) Liu, Z.; Romero-Canelón, I.; Qamar, B.; Hearn, J. M.; Habtemariam, A.; Barry, N. P. E.;
678 Pizarro, A. M.; Clarkson, G. J.; Sadler, P. J. Angew. Chem., Int. Ed. 2014, 53, 3941−3946. (b)
679 Needham, R. J.; Sanchez-Cano, C.; Zhang, X.; Romero-Canelón, I.; Habtemariam, A.; Cooper,
680 M. S.; Meszaros, L.; Clarkson, G. J.; Blower, P. J.; Sadler, P. J. Angew. Chem., Int. Ed. 2017,
681 56, 1017−1020.

682 (6) Wong, D. Y. Q.; Ong, W. W. F.; Ang, W. H. Angew. Chem., Int. Ed. 2015, 54, 6483−6487.

683 (7) Wang, Z.; Xu, Z.; Zhu, G. Angew. Chem., Int. Ed. 2016, 55, 15564−15568.

684 (8) (a) Cutillas, N.; Yellol, G. S.; de Haro, C.; Vicente, C.; Rodríguez, V.; Ruiz, J. Coord. Chem.
685 Rev. 2013, 257, 2784−2797. (b) Montaña, A. M.; Batalla, C. Curr. Med. Chem. 2009, 16,
686 2235−2260.

687 (9) (a) Navarro-Ranninger, C.; López-Solera, I.; González, V. M.; Pérez, J. M.; Alvarez-Valdés, A.;
688 Martín, A.; Raithby, P. R.; Masaguer, J. R.; Alonso, C. Inorg. Chem. 1996, 35, 5181−5187. (b)
689 El-Mehasseb, I. M.; Kodaka, M.; Okada, T.; Tomohiro, T.; Okamoto, K.; Okuno, H. J. Inorg.
690 Biochem. 2001, 84, 157−158. (c) Okada, T.; El-Mehasseb, I. M.; Kodaka, M.; Tomohiro, T.;
691 Okamoto, K.; Okuno, H. J. Med. Chem. 2001, 44, 4661−4667. (d) Edwards, G. L.; Black,
692 D.St.C.; Deacon, G. B.; Wakelin, L. P. G. Can. J. Chem. 2005, 83, 969−979. (e) Edwards, G. L.;
693 Black, D.St.C.; Deacon, G. B.; Wakelin, L. P. G. Can. J. Chem. 2005, 83, 980−989. (f) Ruiz, J.;
694 Cutillas, N.; Vicente, C.; Villa, M. D.; López, G.; Lorenzo, J.; Avilés, F. X.; Moreno, F. V.;
695 Bautista, D. Inorg. Chem. 2005, 44, 7365−7376. (g) Ruiz, J.; Lorenzo, J.; Sanglas, L.; Cutillas,
696 N.; Vicente, C.; Villa, M. D.; Avilés, F. X.; López, G.; Moreno, V.; Pérez, J.; Bautista, D. Inorg.

Chem. 2006, 45, 6347−6360. (h) Ruiz, J.; Rodríguez, V.; Cutillas, N.; López, G.; Bautista, D. Inorg. Chem. 2008, 47, 10025−10036. (i) Ruiz, J.; Lorenzo, J.; Vicente, C.; López, G.; López de Luzuriaga, J. M.; Monge, M.; Avilés, F. X.; Bautista, D.; Moreno, V.; Laguna, A. Inorg. Chem. 2008, 47, 6990−7001. (j) Samouei, H.; Rashidi, M.; Heinemann, F. W. J. Organomet. Chem. 2011, 696, 3764−3771. (k) Albert, J.; Bosque, R.; Crespo, M.; Granell, J.; López, C.; Cortés, R.; González, A.; Quirante, J.; Calvis, C.; Messeguer, R.; Baldomà, L.; Badia, J.; Cascante, M. Bioorg. Med. Chem. 2013, 21, 4210−4217. (l) Ruiz, J.; Vicente, C.; de Haro, C.; Espinosa, A. Inorg. Chem. 2011, 50, 2151−2158. (m) Ruiz, J.; Rodríguez, V.; Cutillas, N.; Espinosa, A.; Hannon, M. J. J. Inorg. Biochem. 2011, 105, 525−531.

(10) (a) Cortés, R.; Crespo, M.; Davin, L.; Martín, R.; Quirante, J.; Ruiz, D.; Messeguer, R.; Calvis, C.; Baldomà, L.; Badia, J.; Font-Bardía, M.; Calvet, T.; Cascante, M. Eur. J. Med. Chem. 2012, 54, 557−566. (b) Ma, D.-L.; Che, C.-M. Chem. - Eur. J. 2003, 9, 6133−6144. (c) Wang, P.; Leung, C.-H.; Ma, D.-L.; Sun, W.R.-Y.; Yan, S.-C.; Chen, Q.-S.; Che, C.-M. Angew. Chem., Int. Ed. 2011, 50, 2554−2558. (d) Quirante, J.; Ruiz, D.; González, A.; López, C.; Cascante, M.; Cortés, R.; Messeguer, R.; Calvis, C.; Baldomà, L.; Pascual, A.; Guérardel, Y.; Pradines, B.; Font-Bardia, M.; Calvet, T.; Biot, C. J. Inorg. Biochem. 2011, 105, 1720−1728. (e) Chellan, P.; Land, K. M.; Shokar, A.; Au, A.; An, S. H.; Clavel, C. M.; Dyson, P. J.; de Kock, C.; Smith, P. J.; Chibale, K.; Smith, G. S. Organometallics 2012, 31, 5791−5799. (f) Escolà, A.; Crespo, M.; Quirante, J.; Cortés, R.; Jayaraman, A.; Badía, J.; Baldomà, L.; Calvet, T.; Font-Bardía, M.; Cascante, M. Organometallics 2014, 33, 1740−1750.

(11) Omae, I. Coord. Chem. Rev. 2014, 280, 84−95.

(12) (a) Avshu, A.; O'Sullivan, R. O.; Parkins, A. W.; Alcock, N. W.; Countryman, R. M. J. Chem. Soc., Dalton Trans. 1983, 1619−1624. (b) Capapé, A.; Crespo, M.; Granell, J.; Font-Bardia, M.; Solans, X. Dalton Trans. 2007, 2030−2039.

(13) Calmuschi-Cula, B.; Englert, U. Organometallics 2008, 27, 3124−3130.

(14) Martín, R.; Crespo, M.; Font-Bardia, M.; Calvet, T. Polyhedron 2009, 28, 1369−1373.

(15) (a) Albrecht, M. Chem. Rev. 2010, 110, 576−63. (b) Albert, J.; Ariza, X.; Calvet, T.; Font-Bardia, M.; Garcia, J.; Granell, J.; Lamela, A.; López, B.; Martinez, M.; Ortega, L.; Rodriguez, A.; Santos, D. Organometallics 2013, 32, 649−659.

(16) Bednarski, P. J.; Ehrensperger, E.; Schönenberger, H.; Burgemeister, T. Inorg. Chem. 1991, 30, 3015−3025.

(17) (a) López, B.; Rodríguez, A.; Santos, D.; Albert, J.; Ariza, X.; García, J.; Granell, J. Chem. Commun. 2011, 47, 1054−1056. (b) Albert, J.; Cadena, J. M.; González, A.; Granell, J.; Solans, X.; Font-Bardia, M. Chem. Commun. 2003, 528−529. (c) Albert, J.; Cadena, J. M.; González, A.; Granell, J.; Solans, X.; Font-Bardia, M. Chem. - Eur. J. 2006, 12, 887−894. (d) Duran, E.; Gordo, E.; Granell, J.; Font-Bardıa, M.; Solans, X.; Velasco, D.; Lopez-Calahorra, F. Tetrahedron: Asymmetry 2001, 12, 1987−1997. (e) Albert, J.; Crespo, M.; Granell, J.; Rodríguez, J.; Calvet, T.; Zafrilla, J.; Font-Bardia, M.; Solans, X. Organometallics 2010, 29, 214−225.

(18) Vicente, J.; Saura-Llamas, I. Comments Inorg. Chem. 2007, 28, 39−72.

(19) (a) Albert, J.; Bosque, R.; Crespo, M.; Granell, J.; López, C.; Martín, R.; González, A. J.; Jayaraman, A.; Quirante, J.; Calvis, C.; Badía, J.; Baldomà, L.; Font-Bardia, M.; Cascante, M.; Messeguer, R. Dalton Trans. 2015, 44, 13602−13614. (b) Cutillas, N.; Martínez, A.; Yellol, G. S.; Rodriguez, V.; Zamora, A.; Pedreño, M.; Donaire, A.; Janiak, C.; Ruiz, J. Inorg. Chem. 2013, 52, 13529−13535.

(20) (a) Cametti, M.; Crousse, B.; Metrangolo, P.; Milani, R.; Resnati, G. Chem. Soc. Rev. 2012, 41, 31−42. (b) Hagmann, W. K. J. Med. Chem. 2008, 51, 4359−4369.

(21) Pregosin, P. S.; Kunz, R. W. In 31P and 13C NMR of Transition Metal Phosphine Complexes; Diehl, P., Fluck, E., Kosfeld, R., Eds.; Springer-Verlag: Berlin, 1979.

(22) (a) Cook, R. L.; Morse, J. G. Inorg. Chem. 1982, 21, 4103−4105. (b) Marr, A. C.; Nieuwenhuyzen, M.; Pollock, C. L.; Saunders, G. S. Inorg. Chem. Commun. 2006, 9, 407−409.

(23) (a) Crespo, M.; Font-Bardia, M.; Calvet, T. Dalton Trans. 2011, 40, 9431−9438. (b) Ruiz, J.; Cutillas, N.; Villa, M. D.; López, G.; Espinosa, A.; Bautista, D. Dalton Trans. 2009, 9637−9644. (c) Ruiz, J.; Rodríguez, V.; Cutillas, N.; López, G.; Bautista, D. Inorg. Chem. 2008, 47, 10025−10036. (d) Martin, R.; Crespo, M.; Font-Bardia, M.; Calvet, T. Organometallics 2009, 28, 587−597. (e) Anderson, C. M.; Crespo, M.; Kfoury, N.; Weinstein, M. A.; Tanski, J. M. Organometallics 2013, 32, 4199−4207. (f) Albert, J.; Granell, J.; Zafrilla, J.; Font-Bardia, M.; Solans, X. J. Organomet. Chem. 2005, 690, 422−429. (g) Albert, J.; Granell, J.; Luque, A.; Minguez, J.; Moragas, R.; Font-Bardia, M.; Solans, X. J. Organomet. Chem. 1996, 522, 87−95. (h) Doherty, S.; Knight, J. G.; Ward, N. A. B.; Bittner, D. M.; Wills, C.; McFarlane, W.; Clegg, W.; Harrington, R. W. Organometallics 2013, 32, 1773−1788.

(24) Granell, J.; Martínez, M. Dalton Trans. 2012, 41, 11243−11258.

(25) Crespo, M.; Font-Bardía, M.; Granell, J.; Martínez, M.; Solans, X. Dalton Trans. 2003, 3763−3769.

(26) Crespo, M.; Martínez, M.; Nabavizadeh, S. M.; Rashidi, M. Coord. Chem. Rev. 2014, 279, 115−140.

(27) Albert, J.; Granell, J.; Sales, J.; Solans, X.; Font-Altaba, M. Organometallics 1986, 5, 2567−2568.

(28) Crespo, M.; Martínez, M.; Sales, J.; Solans, X.; Font-Bardía, M. Organometallics 1992, 11, 1288−1295.

(29) Crespo, M.; Martínez, M.; de Pablo, E. J. Chem. Soc., Dalton Trans. 1997, 1231−1235.

(30) Font, H.; Font-Bardia, M.; Gomez, K.; González, G.; Granell, J.; Macho, I.; Martínez, M. Dalton Trans. 2014, 43, 13525−13536.

(31) Favier, I.; Gómez, M.; Granell, J.; Martínez, M.; Font-Bardía, M.; Solans, X. Dalton Trans. 2005, 123−132.

(32) Gómez, M.; Granell, J.; Martínez, M. Eur. J. Inorg. Chem. 2000, 2000, 217−224.

(33) (a) Hall, M. D.; Telma, K. A.; Chang, K.-E.; Lee, T. D.; Madigan, J. P.; Lloyd, J. R.; Goldlust, I. S.; Hoeschele, J. D.; Gottesman, M. M. Cancer Res. 2014, 74, 3913−3922. (b) Kerrison, S. J. S.; Sadler, P. J. J. Chem. Soc., Chem. Commun. 1977, 861−863.

(34) Bose, R. N.; Maurmann, L.; Mishur, R. J.; Yasui, L.; Gupta, S.; Grayburn, W. S.; Hofstetter, H.; Salley, T. Proc. Natl. Acad. Sci. U. S. A. 2008, 105, 18314−18319.

(35) Pommier, Y.; Leo, E.; Zhang, H.-L.; Marchand, C. Chem. Biol. 2010, 17, 421−433.

(36) Malina, J.; Farrell, N. P.; Brabec, V. Angew. Chem., Int. Ed. 2014, 53, 12812−12816.

(37) Neves, A. P.; Pereira, M. X. G.; Peterson, E. J.; Kipping, R.; Vargas, M. D.; Silva, F. P., Jr.; Carneiro, J. W. N.; Farrell, N. P. J. Inorg. Biochem. 2013, 119, 54−64.

(38) Zou, T.; Liu, J.; Lum, C. T.; Ma, C.; Chan, R.C.-T.; Lok, C. N.; Kwok, W.-M.; Che, C.-M. Angew. Chem., Int. Ed. 2014, 53, 10119− 10123.

(39) Fricker, S. P. Metallomics 2010, 2, 366−377.

785 (40) Spencer, J.; Casini, A.; Zava, O.; Rathnam, R. P.; Velhanda, S. K.; Pfeffer, M.; Callear, S. K.;
786 Hursthouse, M. B.; Dyson, P. J. Dalton Trans. 2009, 10731−10735.

787 (41) Malumbres, M.; Barbacid, M. Cancer Cell 2006, 9, 2−4.

788 (42) Schafer, Z. T.; Grassian, A. R.; Song, L.; Jiang, Z.; Gerhart-Hines, Z.; Irie, H. Y.; Gao, S.;
789 Puigserver, P.; Brugge, J. S. Nature 2009, 461, 109−113.

790 (43) Miyajima, A.; Nakashima, J.; Yoshioka, K.; Tachibana, M.; Tazaki, H.; Murai, M. Br. J. Cancer
791 1997, 76, 206−210.

792 (44) Ozben, T. J. Pharm. Sci. 2007, 96, 2181−2196.

793 (45) Tarrado-Castellarnau, M.; Cortés, R.; Zanuy, M.; Tarragó-Celada, J.; Polat, I. H.; Hill, R.; Fan,
794 T. W. M.; Link, W.; Cascante, M. Pharmacol. Res. 2015, 102, 218−234.

795 (46) Liu, J.; Zhang, C.; Hu, W.; Feng, Z. Cancer Lett. 2015, 356, 197−203.

796 (47) Ritacco, I.; Russo, N.; Sicilia, E. Inorg. Chem. 2015, 54, 10801−10810.

797 (48) Vicente, J.; Abad, J. A.; Frankland, A. D.; Ramirez de Arellano, M. C. Chem. - Eur. J. 1999, 5,
798 3066−3075.

799 (49) Perrin, D. D.; Armarego, W. L. F. Purification of Laboratory Chemicals, 5th ed.; Butterworth-
800 Heinemann: Oxford, U.K., 2002.

801 (50) Price, J. H.; Williamson, A. N.; Schramm, R. F.; Wayland, B. B. Inorg. Chem. 1972, 11,
802 1280−1284.

803 (51) Capapé, A.; Crespo, M.; Granell, J.; Vizcarro, A.; Zafrilla, J.; Font-Bardía, M.; Solans, X.
804 Chem. Commun. 2006, 4128−4130.

805 (52) Sheldrick, G. M. Acta Crystallogr., Sect. A: Found. Crystallogr. 2008, 64, 112−122.

806 (53) Binstead, R. A.; Zuberbuhler, A. D.; Jung, B. SPECFIT32, 3.0.34; Spectrum Software
807 Associates: Marlborough, MA, 2005.

808 (54) Maeder, M.; King, P. ReactLab; Jplus Consulting Pty Ltd: East Fremantle, West Australia,
809 Australia, 2009

810 (55) Roiban, G. D.; Serrano, E.; Soler, T.; Aullón, G.; Grosu, I.; Cativiela, C.; Martínez, M.;
811 Urriolabeitia, E. P. Inorg. Chem. 2011, 50, 8132−8143.

(56) Mosmann, T. J. Immunol. Methods 1983, 65, 55−63.

(57) Matito, C.; Mastorakou, F.; Centelles, J. J.; Torres, J. L.; Cascante, M. Eur. J. Nutr. 2003, 42, 43−49.

(58) Abdullah, A.; Huq, F.; Chowdhury, A.; Tayyem, H.; Beale, P.; Fisher, K. BMC Chem. Biol. 2006, 6, 3.

(59) Sappal, D. S.; McClendon, A. K.; Fleming, J. A.; Thoroddsen, V.; Connolly, K.; Reimer, C.; Blackman, R. K.; Bulawa, C. E.; Osheroff, N.; Charlton, P.; Rudolph-Owen, L. Mol. Cancer Ther. 2004, 3, 47−58.

(60) Casini, A.; Gabbiani, C.; Sorrentino, F.; Rigobello, M. P.; Bindoli, A.; Geldbach, T. J.; Marrone, A.; Re, N.; Hartinger, C. G.; Dyson, P. G.; Messori, L. J. Med. Chem. 2008, 51, 6773−6781.

(61) Spartan ’14; Wavefunction, Inc.: Irvine, CA, 2014.

(62) Halgren, T. A. J. Comput. Chem. 1996, 17, 490−519.

(63) (a) Becke, A. D. J. Chem. Phys. 1993, 98, 5648−5652. (b) Lee, C.; Yang, W.; Parr, R. G. Phys. Rev. B: Condens. Matter Mater. Phys. 1988, 37, 785−789.

(64) Frisch, M. J.; Trucks, G. W.; Schlegel, H. B.; Scuseria, G. E.; Robb, M. A.; Cheeseman, J. R.; Scalmani, G.; Barone, V.; Mennucci, B.; Petersson, G. A.; Nakatsuji, H.; Caricato, M.; Li, X.; Hratchian, H. P.; Izmaylov, A. F.; Bloino, J.; Zheng, G.; Sonnenberg, J. L.; Hada, M.; Ehara, M.; Toyota, K.; Fukuda, R.; Hasegawa, J.; Ishida, M.; Nakajima, T.; Honda, Y.; Kitao, O.; Nakai, H.; Vreven, T.; Montgomery, J. A., Jr.; Peralta, J. E.; Ogliaro, F.; Bearpark, M.; Heyd, J. J.; Brothers, E.; Kudin, K. N.; Staroverov, V. N.; Kobayashi, R.; Normand, J.; Raghavachari, K.; Rendell, A.; Burant, J. C.; Iyengar, S. S.; Tomasi, J.; Cossi, M.; Rega, N.; Millam, J. M.; Klene, M.; Knox, J. E.; Cross, J. B.; Bakken, V.; Adamo, C.; Jaramillo, J.; Gomperts, R.; Stratmann, R. E.; Yazyev, O.; Austin, A. J.; Cammi, R.; Pomelli, C.; Ochterski, J. W.; Martin, R. L.; Morokuma, K.; Zakrzewski, V. G.; Voth, G. A.; Salvador, P.; Dannenberg, J. J.; Dapprich, S.; Daniels, A. D.; Farkas, O.; Foresman, J. B.; Ortiz, J. V.; Cioslowski, J.; Fox, D. J. Gaussian 09, revision C.02; Gaussian, Inc.: Wallingford, CT, 2009.

(65) (a) Wadt, W. R.; Hay, P. J. J. Chem. Phys. 1985, 82, 284−298. (b) Hay, P. J.; Wadt, W. R. J. Chem. Phys. 1985, 82, 299−310.

(66) (a) Hehre, W. J.; Ditchfield, R.; Pople, J. A. J. Chem. Phys. 1972, 56, 2257−2261. (b) Hariharan, P. C.; Pople, J. A. Theor. Chim. Acta 1973, 28, 213−222.

(67) (a) Barone, V.; Cossi, M. J. Phys. Chem. A 1998, 102, 1995−2001. (b) Cossi, M.; Rega, N.; Scalmani, G.; Barone, V. J. Comput. Chem. 2003, 24, 669−681.

845 **Legends to figures**

846

847 **Scheme 1.** Synthesis of Platinum(II) Compounds[a]

848

849 **Figure. 1**. Molecular structure of 3. Selected bond lengths (Å) and angles (deg) with estimated standard
850 deviations: Pt(1)−C(8): 2.0255(15); Pt(1)−N(1): 2.1051(14); Pt(1)−P(1): 2.2358(4); Pt(1)−Cl(1):
851 2.4051(4); C(8)−Pt(1)−N(1): 84.90(6); C(8)−Pt(1)−P(1): 95.45(5); N(1)−Pt(1)−Cl(1): 84.09(4);
852 P(1)−Pt(1)−Cl(1): 95.917(14).

853

854 **Figure. 2**. Eyring plot of the temperature dependence of the rate constants obtained for the C−H bond
855 activation process measured.

856

857 **Figure. 3**. Interaction of pBluescript SK+ plasmid DNA (0.8 μg) with increasing concentrations of
858 compounds under study 2−6, cisplatin, and ethidium bromide (EB). Lane 1: DNA only. Lane 2: 2.5 μM.
859 Lane 3: 5 μM. Lane 4: 10 μM. Lane 5: 25 μM. Lane 6: 50 μM. Lane 7: 75 μM. Lane 8: 100 μM. Lane 9:
860 200 μM; sc = supercoiled closed circular DNA; oc = open circular DNA.

861

862 **Figure. 4** Effect of compounds 5 and 6 on topoisomerase I mediated relaxation at different
863 concentrations. Conversion of supercoiled pBluescript plasmid DNA (0.8 μg) to relaxed DNA by the
864 action of topoisomerase I (3 units) in the absence or in the presence of increasing amounts of
865 compounds 5 and 6 was analyzed by agarose gel electrophoresis. Ethidium bromide (EB) was used as a
866 control of intercalating agent and etoposide (E) as a control of nonintercalating agent. Lane 1: (−)
867 scDNA only. Lane 2: 0 μM drug. Lane 3: 10 μM drug. Lane 4: 25 μM drug. Lane 5: 50 μM drug. Lane
868 6: 100 μM drug. Except for lane 1, all lanes included topoisomerase I; sc = supercoiled closed circular
869 DNA; oc = open circular DNA.

870

871 **Figure. 5**. Effect of compound 5 on the activity of topoisomerase I. Lane 1: (−) scDNA as a control.
872 Lane 2: relaxed DNA as a control. Relaxed pBluescript plasmid DNA was incubated with topoisomerase
873 I (3 units) in the presence of 25 μM (lane 4), 50 μM (lane 5), or100 μM (lane 6) of compound 5, and 10
874 μM (lane 3) of EB. The conversion of relaxed DNA to supercoiled DNA was analyzed after a 20 min
875 incubation. Reaction containing EB is included as an example of an intercalative drug. sc = supercoiled
876 closed circular DNA; oc = open circular DNA.

877

878 **Figure. 6**. Percentage of cell cycle distribution in A-549 cells. The conditions include untreated cells
879 (control) and cells treated with compounds 3, 5, or 6 at concentrations equal to their IC50 values (7.0,

880 0.28, and 0.73 μM, respectively) for 72 h. The harvested cells were stained with PI (propidium iodide)
881 and their DNA content analyzed by flow cytometry.
882
883 **Figure 7.** Percentage variations of A-549 which are in alive (Q4), early apoptotic (Q3), or late
884 apoptotic/necrotic (Q2/Q1) phases. The conditions include untreated cells (control) and the cells treated
885 with compounds 3, 5 or 6 at a concentration equal to their IC50 value (7.0, 0.28, and 0.73 μM,
886 respectively) for 72 h. The harvested cells were stained with Annexin-PI and analyzed by flow
887 cytometry.
888
889 **Figure 8.** ROS levels after 24, 48, and 72 h of incubation with compounds 3−6 at their IC50
890 concentrations (7.0, 8.13, 0.28, and 0.73 μM, respectively) in A-549 lung adenocarcinoma cell line.
891
892 **Figure 9**. Western Blot analysis of certain proteins after 24 h of incubation with compounds 3, 5, or 6 at
893 their IC50 concentrations or double of IC50 concentrations in A-549 lung adenocarcinoma cell line.
894
895 **Scheme 2**. Plausible Mechanism for the Platinum(II) Catalytic Oxidation Process
896

SCHEME 1

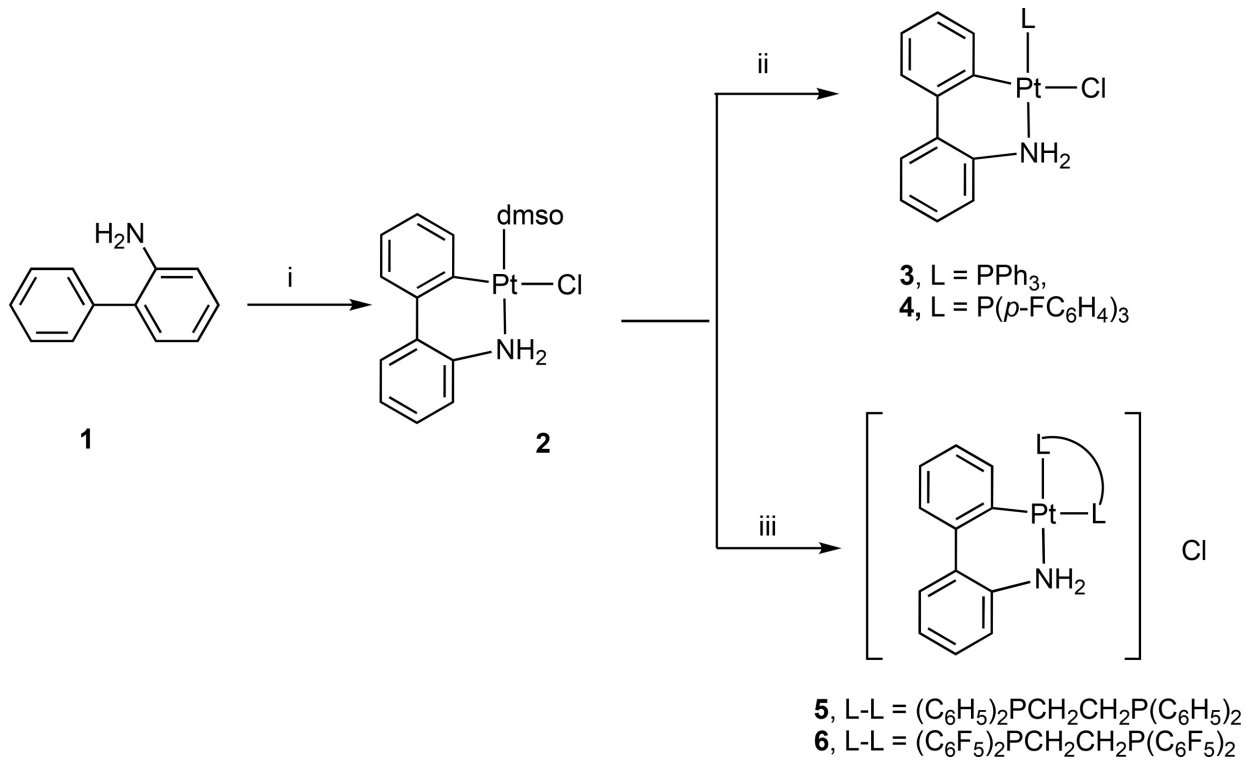
H2N
i
dmso
Pt
Cl
NH2
1
2
ii
iii
L
Pt
Cl
NH2
3, L = PPh3,
4, L = P(p-FC6H4)3
L
Pt
L
NH2
Cl
5, L-L = (C6H5)2PCH2CH2P(C6H5)2
6, L-L = (C6F5)2PCH2CH2P(C6F5)2

FIGURE 1

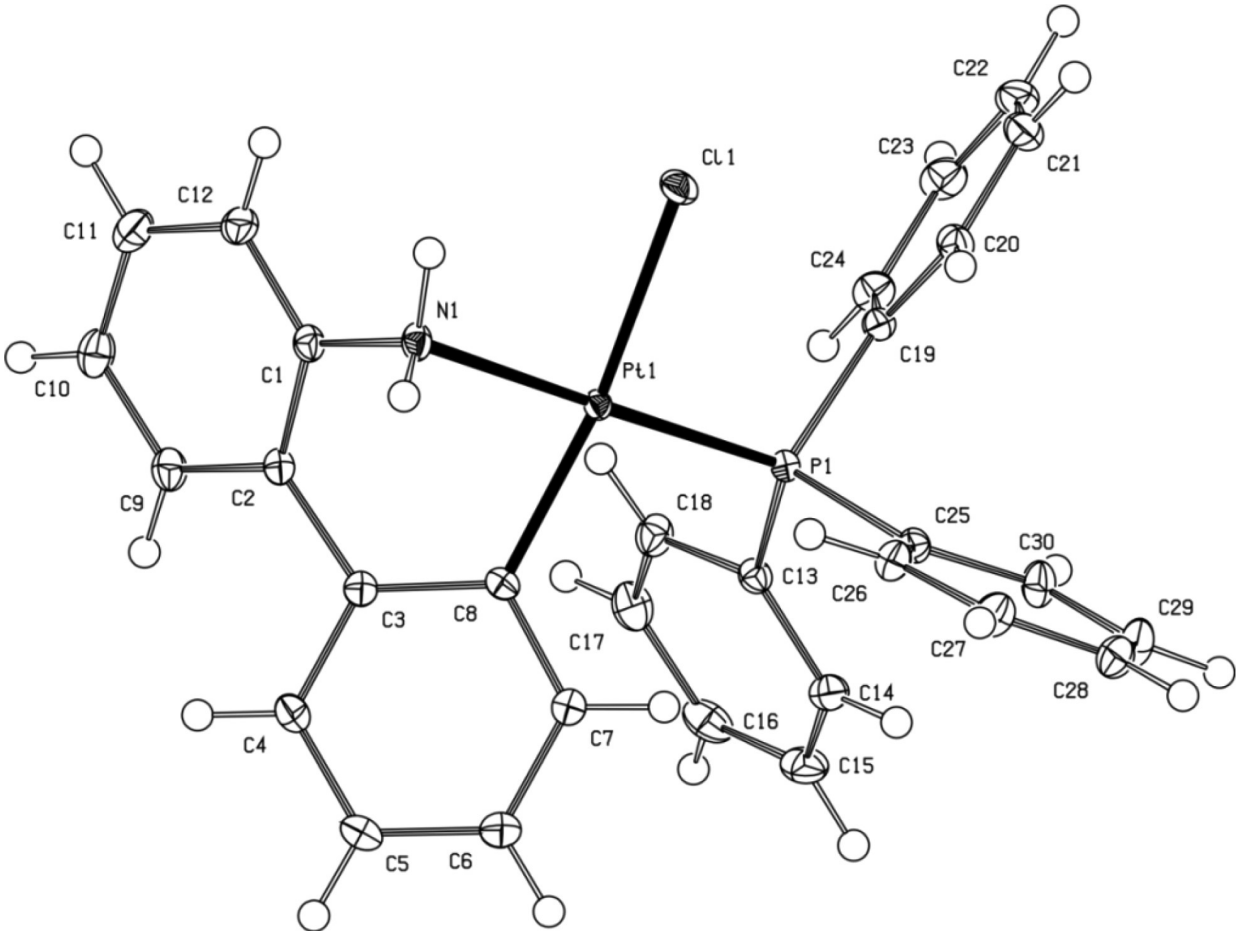
C22
C23
C21
Cl1
C12
C11
C20
C24
N1
C19
C10
C1
Pt1
P1
C9
C2
C18
C25
C30
C13
C26
C3
C8
C29
C17
C27
C14
C28
C16
C4
C7
C15
C5
C6

907 **FIGURE 2**

908

909

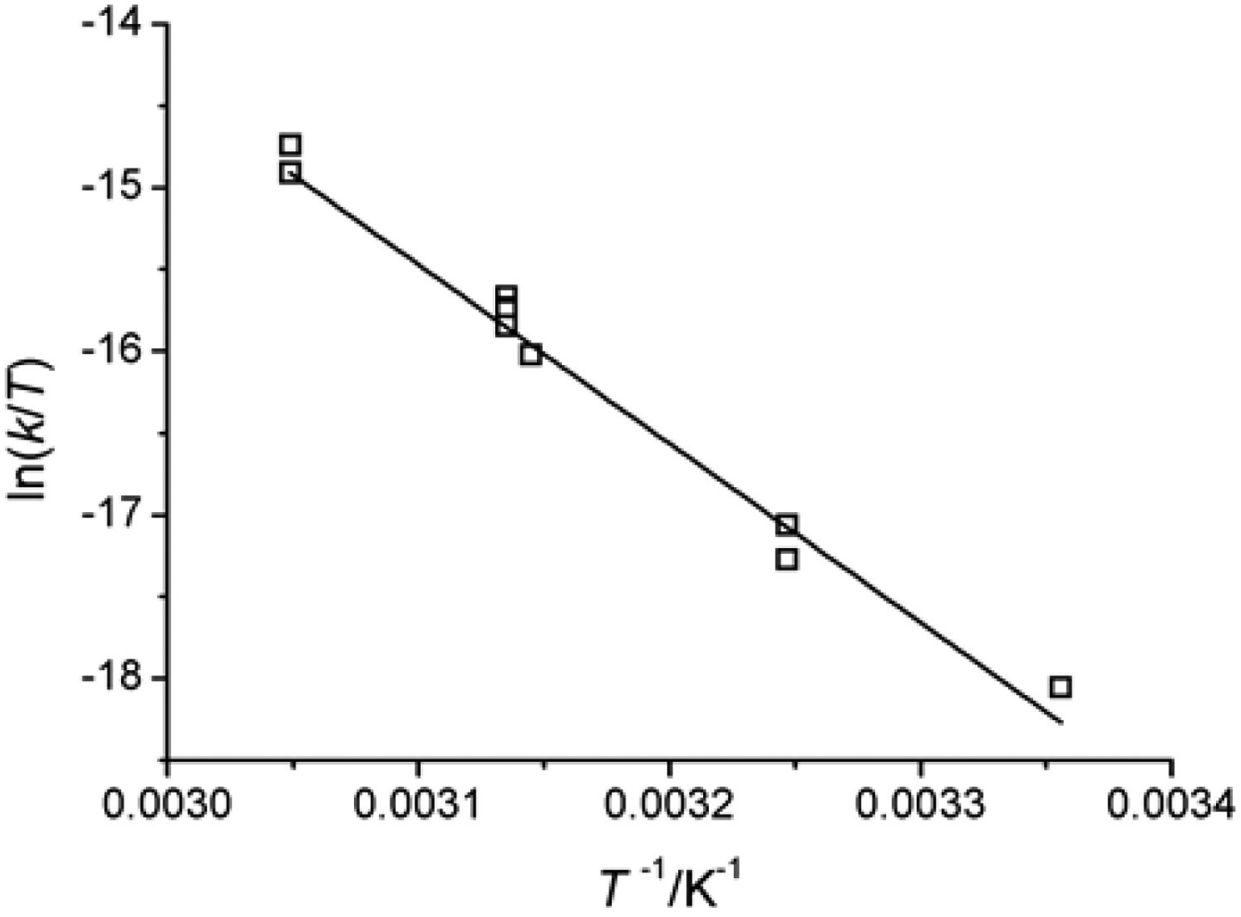

910

911

912 **FIGURE 3**

913

914

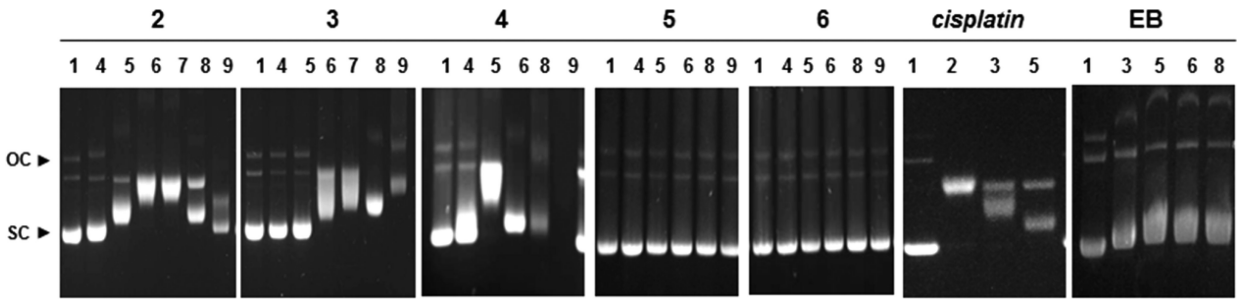

915

916

FIGURE 4

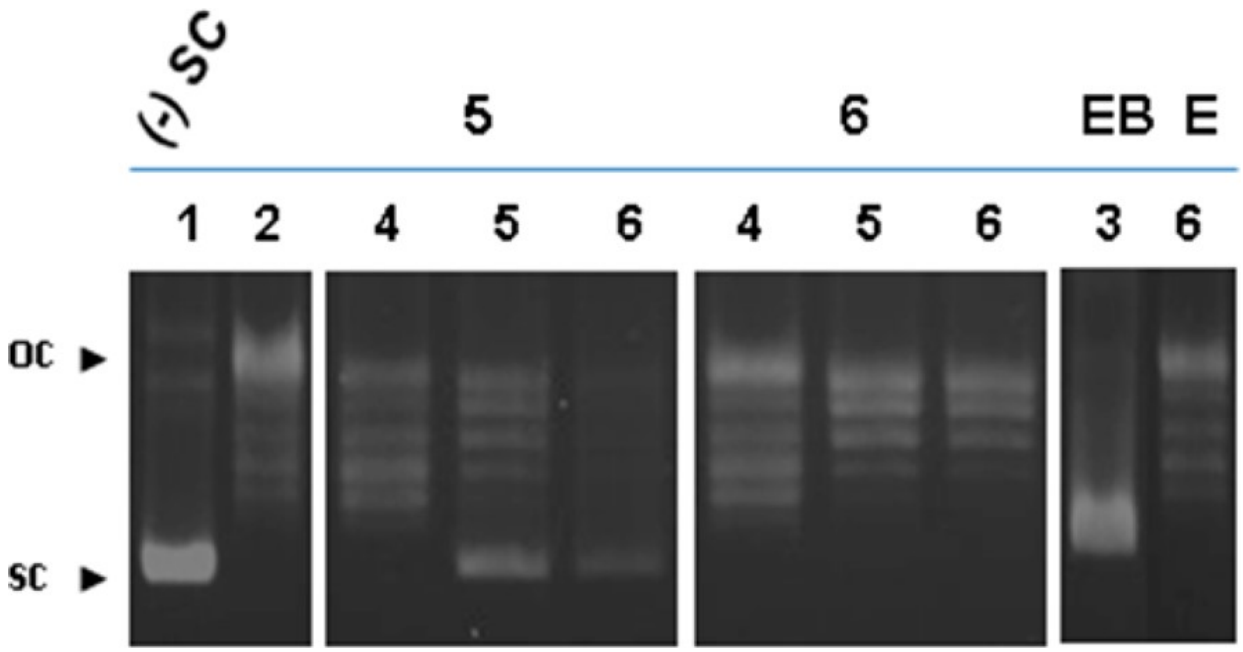

FIGURE 5

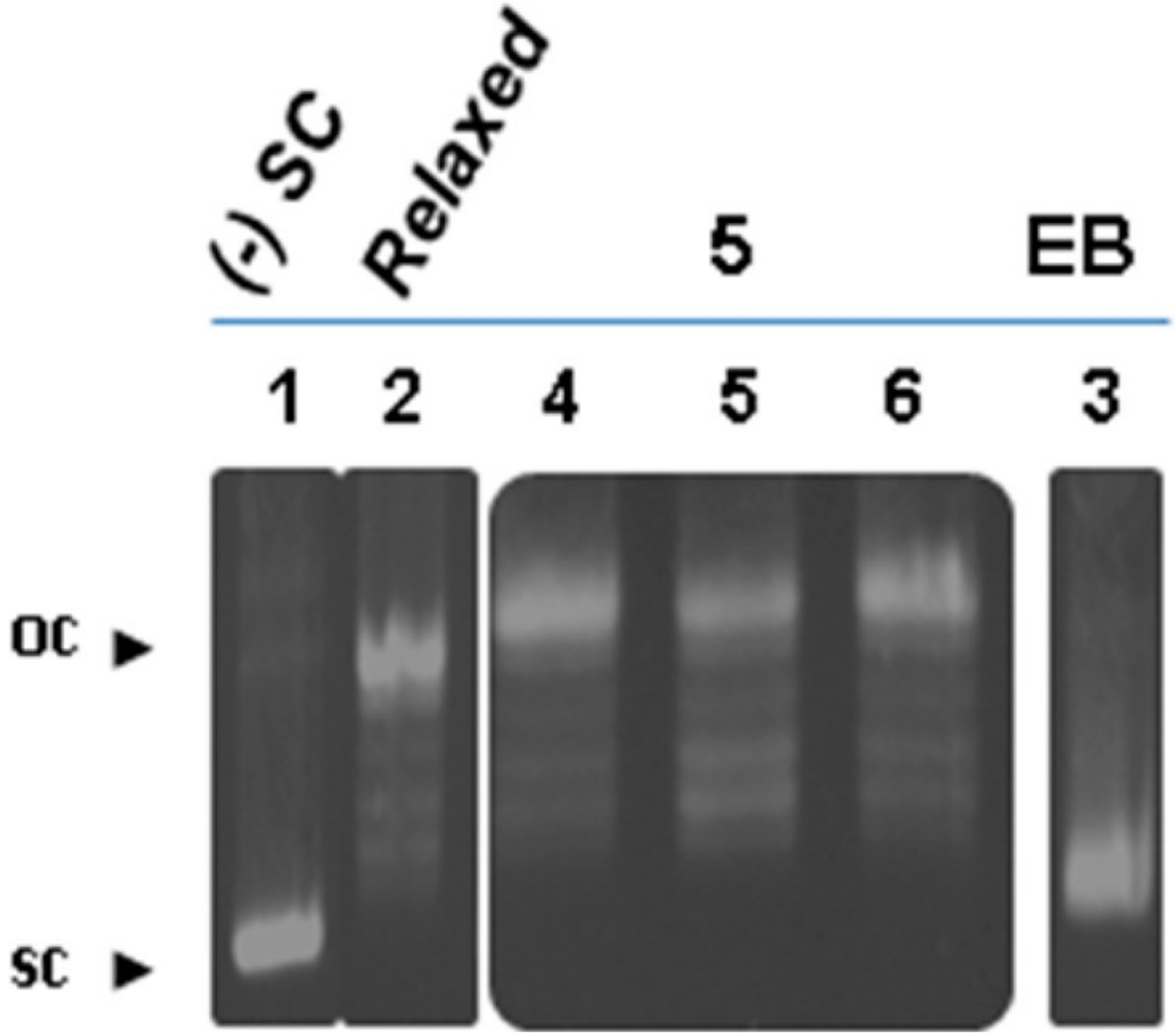

927 **FIGURE 6**

928

929

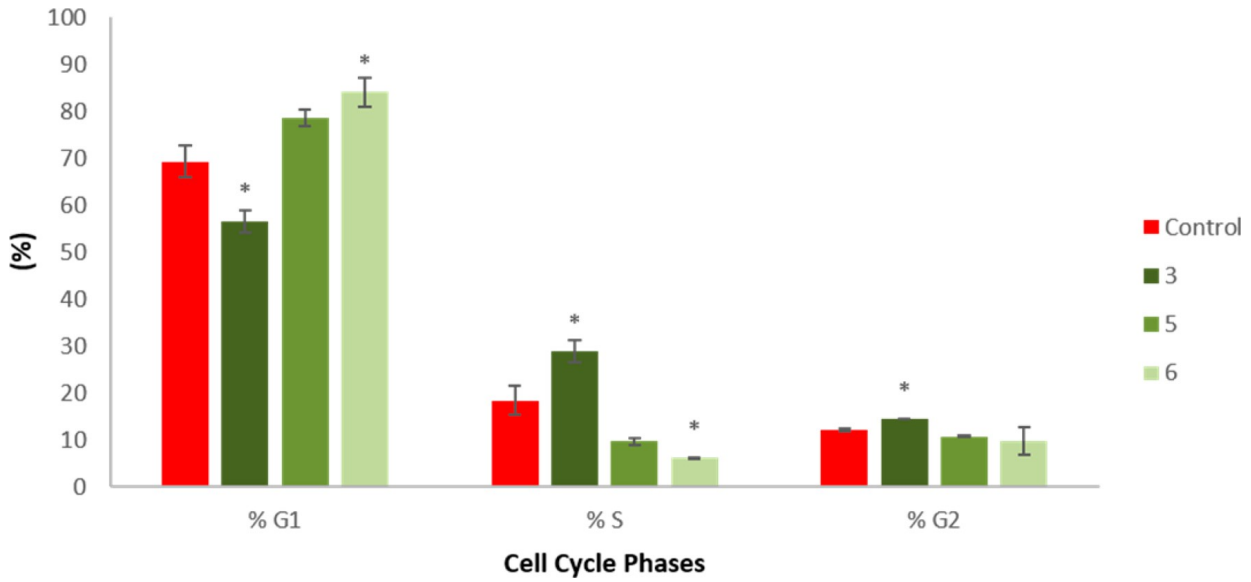

930

931

932 **FIGURE 7**

933

934

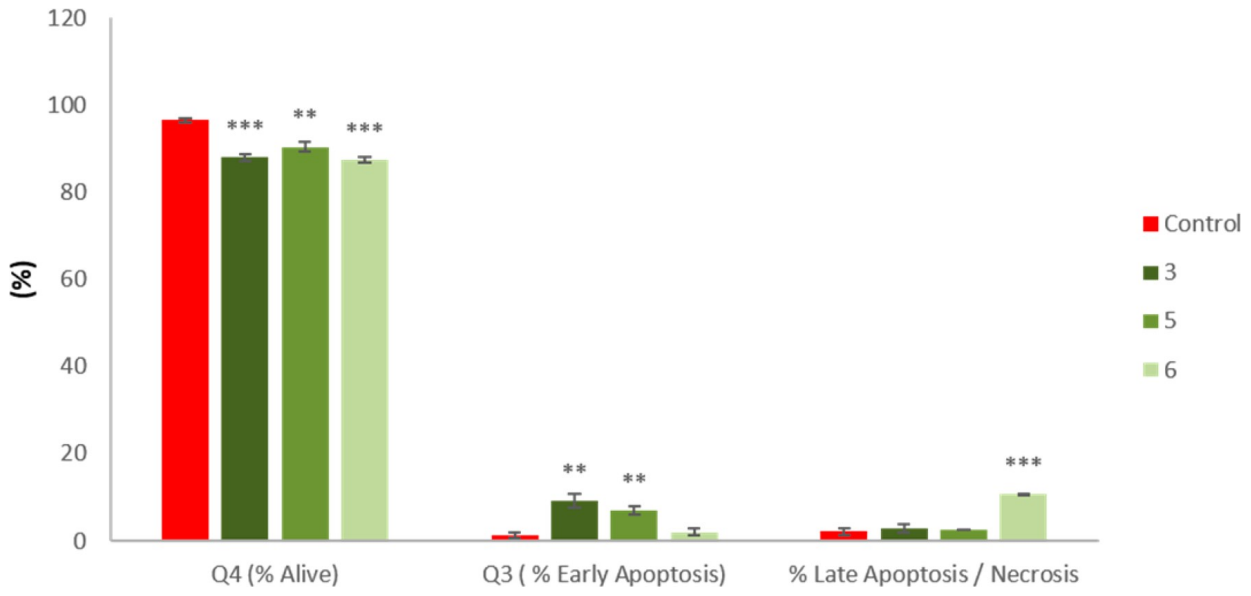

935

936

937 **FIGURE 8**

938

939

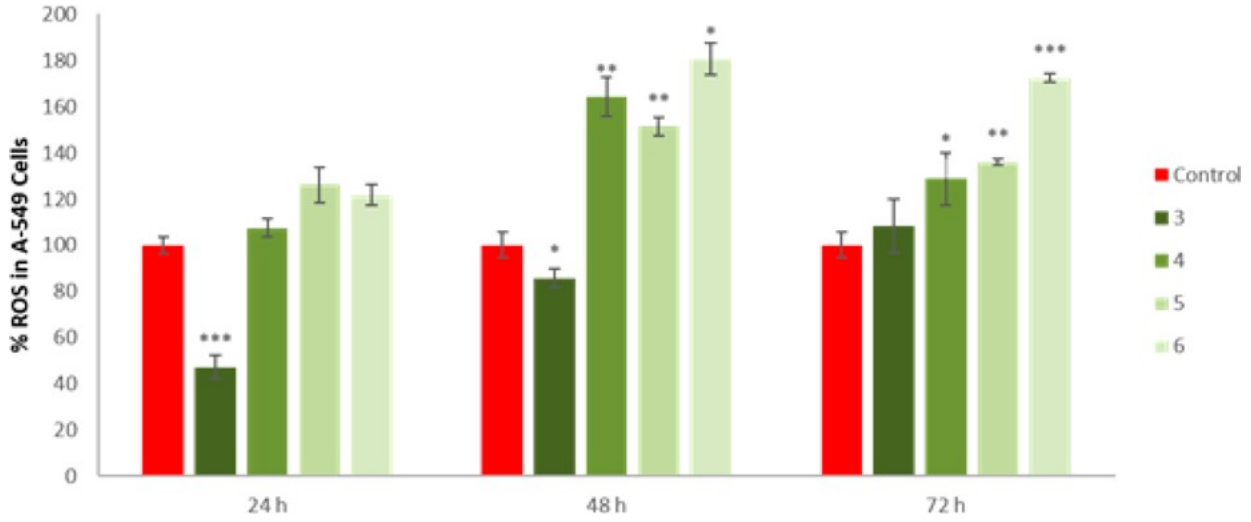

940

941

942 **FIGURE 9**

943

944 .

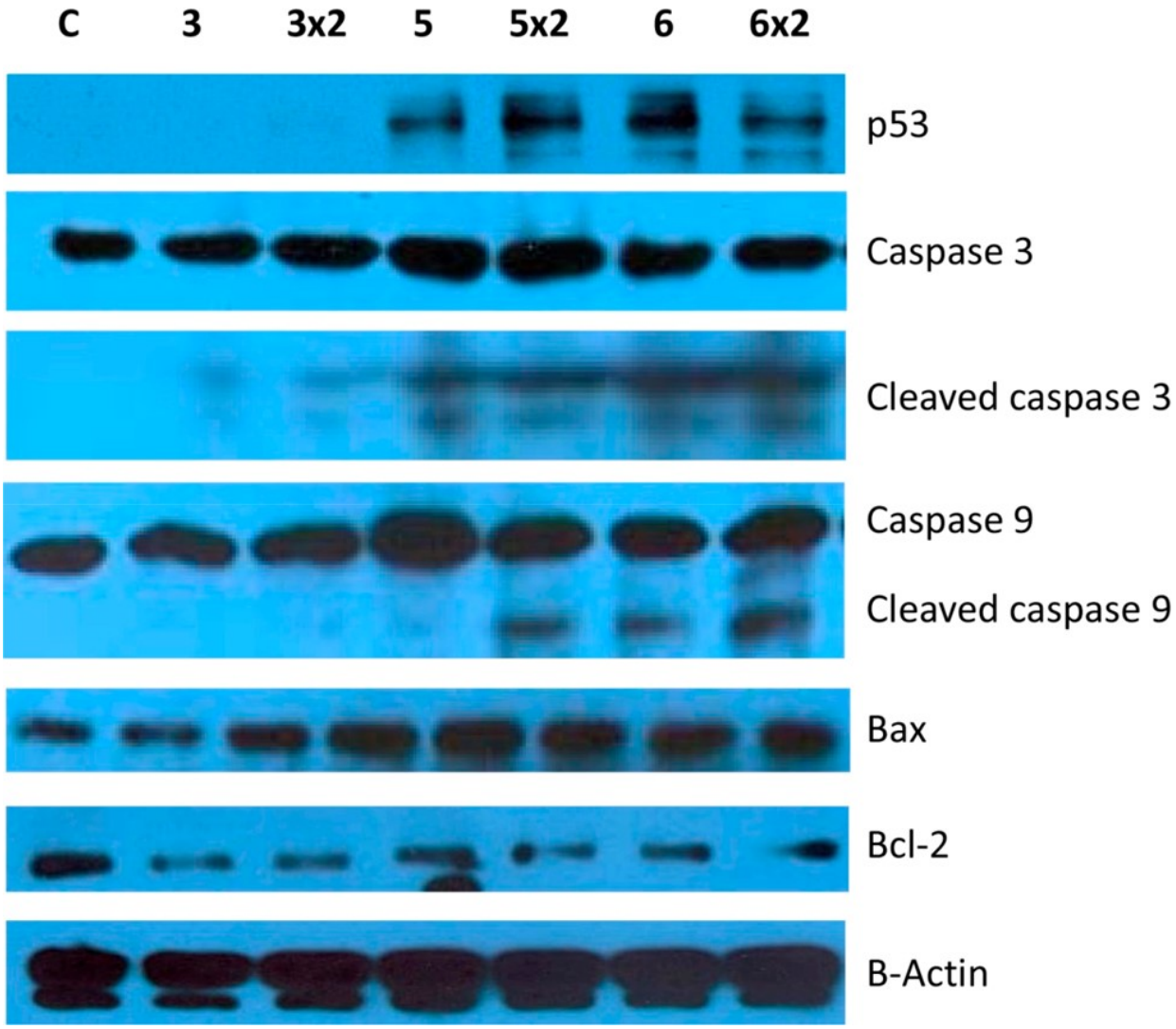

945

946

SCHEME 2

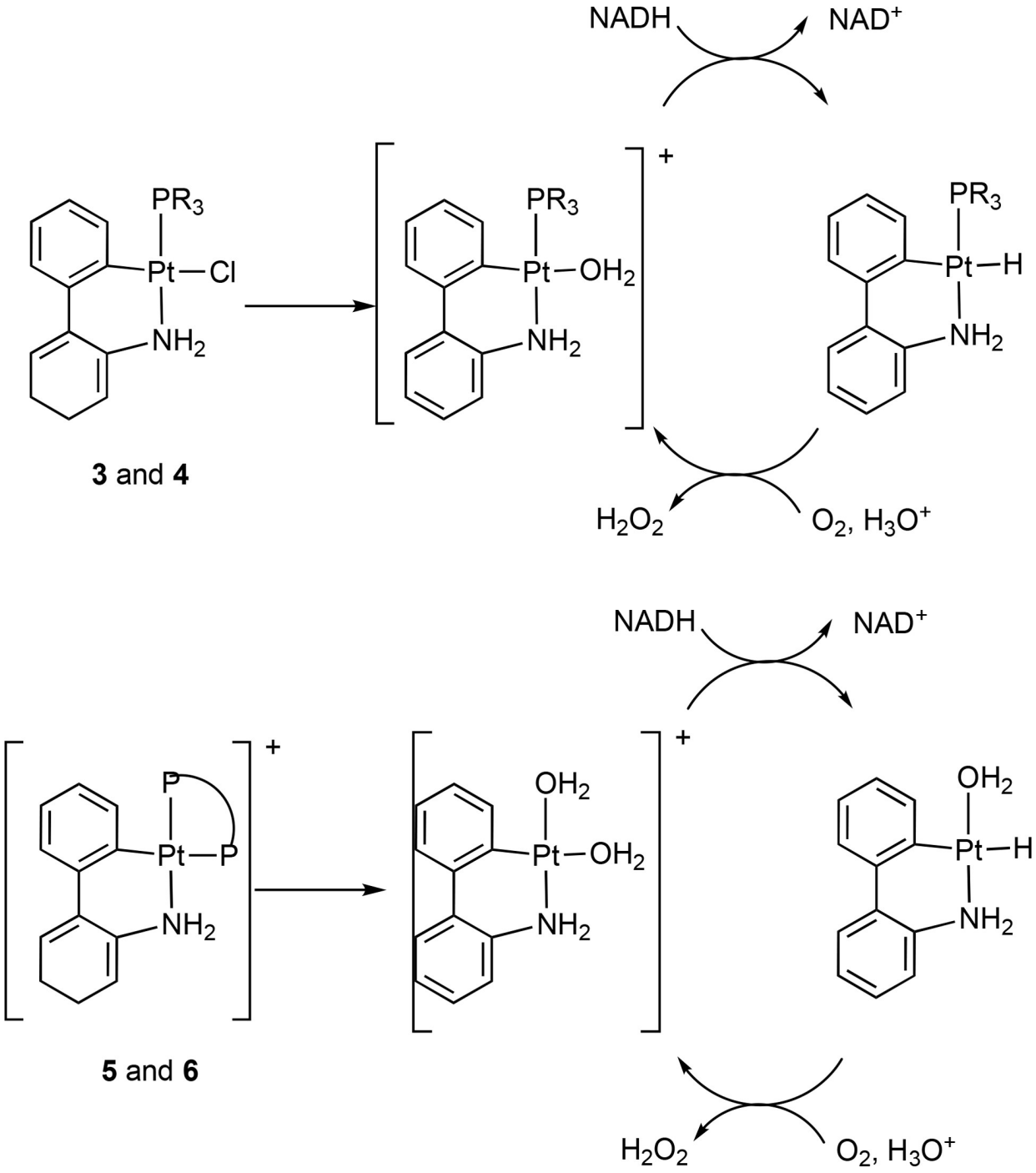
NADH
NAD+
PR3
Pt—Cl
NH2
PR3
Pt—OH2
NH2
+
PR3
Pt—H
NH2
3 and 4
H2O2
O2, H3O+
NADH
NAD+
P
Pt—P
NH2
+
OH2
Pt—OH2
NH2
+
OH2
Pt—H
NH2
5 and 6
H2O2
O2, H3O+

952

953 **Table 1**.. IC_{50} (μM) Values for Compounds under Study[a]

954

comp.	A-549	MDA-MB-231	MCF-7	HCT-116	BJ
2	>100	36 ± 11	42 ± 21	17 ± 3	nd
3	7.0 ± 0.1	5.9 ± 0.9	9.4 ± 1.0	7.9 ± 0.8	13 ± 2.1
4	8.13 ± 0.3	2.5 ± 0.2	4.1 ± 0.2	4.2 ± 0.4	11 ± 1.4
5	0.28 ± 0.04	0.6 ± 0.07	0.3 ± 0.02	0.3 ± 0.01	2.7 ± 0.04
6	0.73 ± 0.01	0.3 ± 0.02	0.4 ± 0.04	0.3 ± 0.01	2.3 ± 0.18
cisplatin	9.3 ± 3	11.5 ± 2.4	9.7 ± 1.7	21.1 ± 1.34	8.3 ± 0.7

955 [a]Data are shown as the mean values of two experiments performed in triplicate with the corresponding standard deviations. nd: not determined.